Journal of Neuroinflammation

RESEARCH

Open Access

Translational evidence for increased central amygdala IL-6 activity in alcohol dependence

Celsey M. St. Onge[1†], Chloe Erikson[1†], Bryan Cruz[1,2], Vittoria Borgonetti[1,3], Joel G. Hashimoto[4,5], Jessica A. Cucinello-Ragland[6], Taylor Fitzpatrick-Schmidt[6], Larry Rodriguez[1], Sophia Khom[1,7], Michela Palmisano[1], Roman Vlkolinsky[1], Christopher S. Oleata[1], Tali Nadav[8], Nihal A. Salem[9], Scott Edwards[6], R. Dayne Mayfield[9], Marina Guizzetti[4,5], Amanda J. Roberts[8], Michal Bajo[1] and Marisa Roberto[1,8*]

Abstract

Alcohol use disorder (AUD) is one of the most prevalent mental health disorders worldwide yet effective therapeutics remain limited. Mounting evidence indicates that dysregulated immune signaling in the brain plays a role in AUD pathophysiology. Activation of pro-inflammatory pathways like the interleukin-6 (IL-6) pathway represents a potential point of convergence between synaptic dysfunction and motivational changes in AUD that remain undiscovered. Thus, using a translational neuroscience approach and well-established model of chronic alcohol intake, we investigated the cell-type specific role of IL-6 signaling in the central amygdala, a critical region in the development and maintenance of alcohol dependence. We demonstrate that chronic alcohol exposure recruits IL-6-related pathways in humans and rodents via astrocytic, neuronal, and microglial mechanisms, and that IL-6 inhibits central amygdala GABAergic transmission. Notably, systemic administration of an IL-6 receptor antibody decreased alcohol drinking in alcohol-dependent female mice. Collectively, our findings support IL-6 inhibition as a novel-neuroimmune-targeted therapeutic strategy to reduce excessive drinking in the context of AUD.

Keywords Human, Mouse, Cytokine, Ethanol, Electrophysiology, Gene expression, RNA-seq, RNAscope, Brain, Neuroimmune

[†]Celsey M. St. Onge and Chloe Erikson contributed equally to this work.

*Correspondence:
Marisa Roberto
mroberto@scripps.edu
[1]Department of Translational Medicine, The Scripps Research Institute, 10550 N. Torrey Pines Rd, La Jolla, CA, USA
[2]Department of Pharmacology, Addiction Science, and Toxicology, The University of Tennessee Health Science Center, Memphis, TN, USA
[3]Department of Molecular and Developmental Medicine, University of Siena, Siena, Italy
[4]Department of Behavioral Neuroscience, Oregon Health & Science University, Portland, OR, USA
[5]VA Portland Health Care System, Portland, OR, USA
[6]Department of Physiology and Comprehensive Alcohol-HIV/AIDS Research Center, Louisiana State University Health, New Orleans, LA, USA
[7]Department of Pharmaceutical Sciences, University of Vienna, Vienna, Austria
[8]Animal Models Core Facility, The Scripps Research Institute, La Jolla, CA, USA
[9]Department of Neuroscience and Waggoner Center for Alcohol and Addiction Research, University of Texas at Austin, Austin, TX, USA

Introduction

Alcohol use disorder (AUD) is a chronic relapsing brain disorder that is characterized by a compulsion to seek and consume alcohol resulting in an inability to control alcohol use and the emergence of negative emotional states including dysphoria, anxiety, and irritability during alcohol withdrawal [1, 2]. AUD is highly prevalent worldwide and frequently comorbid with other psychiatric disorders such as depression and anxiety [3–6]. Converging evidence suggests that these negative affective states are driven in part by neuroadaptations within the central amygdala (CeA), which is comprised of mainly GABAergic neurons, where increased GABAergic signaling contributes to negative reinforcement processes that promote alcohol dependence [7–9]. Despite the high prevalence of AUD, current treatment options are very limited and not universally effective in part due to the heterogeneity of AUD. Thus, further study into the mechanisms underlying AUD is warranted to elucidate the neurobiological basis of the disorder.

Compelling evidence supports a critical role for the neuroimmune system in modulating alcohol-related behaviors in the context of excessive alcohol drinking and the pathogenesis of AUD [10–18]. Chronic alcohol exposure disrupts neuroimmune signaling by producing a persistent pro-inflammatory state in the brain characterized by altered neuroimmune gene expression and increased activation of glial cells, including microglia and astrocytes [19]. Neurons, in addition to microglia and astrocytes, respond to and release neuroimmune factors called cytokines, including, but not limited to IL-6, IL-18, IL-1β, and TNFα [20]. In humans, lifetime alcohol consumption is positively correlated with increases in circulating pro-inflammatory cytokines [11, 21, 22]. However, the specific mechanisms by which neuroimmune system components contribute to the neurobiology of AUD are not fully understood. A neuroimmune system component that has garnered interest for its role in the neurobiology of AUD is the cytokine interleukin-6 (IL-6).

IL-6 is a multifunctional cytokine that exhibits both pro- and anti-inflammatory properties [23, 24]. IL-6 belongs to the IL-6 family of cytokines that use membrane glycoprotein 130 (gp130; also known as IL-6 cytokine family signal transducer, IL6ST) as a signal-transducing receptor subunit. One way by which IL-6 exerts its functions is through pro-inflammatory trans-signaling wherein IL-6 binds to the soluble form of the IL-6 receptor (sIL-6R) that is shed from the membrane and transported to various cell types in the brain that express surface gp130 [24, 25]. The IL-6/sIL-6R complex binds to gp130 and activates intracellular signaling cascades including the Janus Kinase/Signal Transducer and Activator of Transcription (JAK/STAT) pathway, the Mitogen-Activated Protein Kinase (MAPK) pathway, and the Phosphoinositide 3-Kinase/Protein Kinase B (PI3K/AKT) pathway (Fig. 1A). Trans-signaling is the predominant form of IL-6 signaling in the brain and occurs in neurons and glial cells including microglia and astrocytes [26, 27]. One potential point of intervention within this mechanism is the administration of an IL-6 receptor antibody (IL-6R Ab). Il-6R Abs such as Toclizumab, used for treatment of autoimmune and inflammatory conditions, bind to IL-6R preventing the association of IL-6R with IL-6 and thus inhibiting signal transduction (Fig. 1A) [28].

IL-6 plays a key role in AUD-related behaviors across both clinical and preclinical studies [24, 29]. In humans, a polymorphism (174 G/C) of the gene encoding IL-6 (*IL6*) is associated with AUD [30], and blood IL-6 levels correlate with greater craving in alcohol cue and prefrontal cue reactivity tests during both acute and prolonged withdrawal [31–33]. In rodents, alcohol exposure induces brain region-specific changes of transcripts and proteins of both members and regulators of the IL-6 pathway [16, 34–41]. The gene *Il6ra* that encodes the IL-6 receptor subunit (IL-6R) is upregulated in the brain of alcohol-preferring rats [42]. Alcohol-preferring mice show increased whole brain IL-6 cytokine family signal transducer (*Il6st*) and signal transducer and activator of transcription 3 (*Stat3*) expression (genes encoding gp130 and STAT3, respectively) whereas suppressor of cytokine signaling 3 (*Socs3*), a negative regulator of STAT signaling, expression is decreased [43]. In addition, *Il6* null mutant mice exhibit reduced alcohol drinking [44] and resistance to stress-induced depressive-like behaviors [45]. Transgenic mice with elevated astrocyte-derived IL-6 show decreased stress-coping behaviors and increased susceptibility to hyperexcitability in the context of acute alcohol withdrawal [46] that is concomitant with increased neuronal excitability in the CeA [47]. Further, there is decreased *Il6ra* expression in the CeA of microglia-depleted mice which also exhibit reduced alcohol drinking [13].

However, several aspects of the impact of chronic alcohol exposure on IL-6 signaling in the CeA remain poorly understood, including potential cell-type and sex-specific regulation of neuroinflammatory mechanisms, the effects of IL-6 on synaptic GABAergic transmission, and the effects of blocking IL-6 signaling on chronic alcohol-induced behavioral phenotypes. Herein, we investigate the IL-6 pathway including its negative regulator, SOCS3, to unveil potential therapeutic targets to alleviate alcohol-induced neuroinflammation and excessive drinking in the context of alcohol dependence. We analyzed postmortem CeA tissue samples from humans diagnosed with AUD and employed a preclinical mouse model, the chronic-intermittent ethanol two-bottle choice paradigm (CIE-2BC; Fig. 1B), to mechanistically investigate

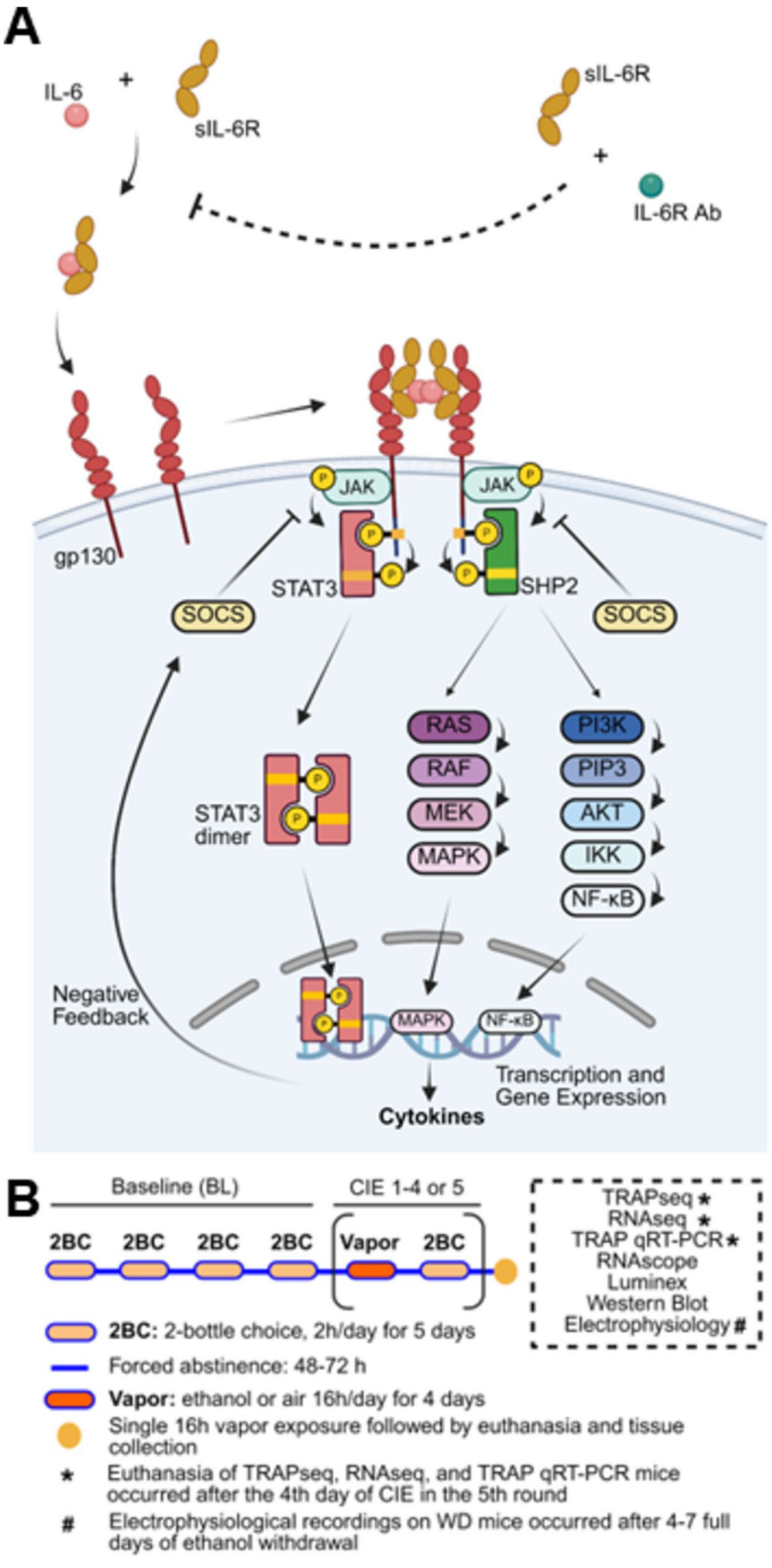

Fig. 1 (See legend on next page.)

(See figure on previous page.)

Fig. 1 IL-6 signaling pathway and overall experimental timeline. **A** IL-6 pro-inflammatory trans-signaling found in neurons, microglia, and astrocytes within the brain. sIL-6R binds to IL-6 which then binds to gp130 (IL6ST) forming the IL-6/IL-6R/gp130 complex. Assembly of this complex leads to activation of intracellular signaling pathways. Presence of IL-6R Ab blocks this signaling by binding to sIL-6R, thus preventing the association of sIL-6R with IL-6 (Created with BioRender.com). **B** The chronic intermittent ethanol – two-bottle choice (CIE-2BC) paradigm was used for all studies in mice. Briefly, alcohol intake (g/kg) is monitored during baseline (BL) two-bottle choice (2BC), and during each 2BC session following vapor/air exposure (total 4–5 rounds of vapor/air-2BC sessions; CIE 1–4 or 5). For full experimental details, please see the methods section

the clinical evidence [37, 48–50]. The CIE-2BC model is a highly translational pre-clinical model for studying AUD, as it captures multiple stages of the disorder: non-dependent alcohol use (Non-Dep; moderate alcohol consumption, voluntary alcohol intake but no alcohol vapor exposure), alcohol dependence (Dep; escalated voluntary alcohol intake following alcohol vapor exposure), and alcohol withdrawal (WD; alcohol dependence followed by 4–7 days of forced abstinence), as well as alcohol naive controls (Naïve; no alcohol exposure) [48, 49, 51–54]. To better understand the neurobiological basis of sex differences in AUD, our clinical and preclinical studies include both sexes [55, 56]. Following CIE-2BC, we utilized RNAseq, qRT-PCR, RNAscope, Luminex assay, and western blot analytical techniques to further elucidate alcohol-induced neuroinflammation in the CeA. To determine specific astrocytic contributions to the dysregulation of IL-6 signaling, we used Aldh1l1-eGFP/Rpl10a mice, which allow for the pull-down of astrocyte-specific RNA using the translating ribosome affinity purification (TRAP) procedure. We then used whole-cell patch clamp electrophysiology recordings from ex vivo mouse CeA slices to assess basal GABAergic transmission, as well as the neuromodulatory role of IL-6 at GABAergic synapses. Finally, we used an IL-6R Ab to evaluate its effect on alcohol dependence-induced escalation of drinking and thus, its potential therapeutic use for AUD.

Material and methods

Animals

Adult male (~25 g) and female (~20 g) hemizygous B6;FBV-Tg(Aldh1l1-EGFP/Rp110a)JD130Htz/J mice (Astrocyte-TRAP), generated by Nathaniel Heintz, [57, 58] were purchased from The Jackson Laboratory (Bar Harbor, ME; strain # 030247; $n = 49$) for TRAP RNAseq and TRAP qRT-PCR studies. Adult male (~30 g) and female (~20 g) C57BL/6 J mice were purchased from The Jackson Laboratory (Bar Harbor, ME; $n = 256$) for RNAscope, multiplex cytokine assay, western blot, electrophysiology and IL-6R Ab treatment studies. Mice were acclimated to the animal facility at The Scripps Research Institute for over one week prior to experimentation. All mice were housed 3–5 per cage with Harlan Teklad Aspen Sani-Chip bedding (#7090A) in light (12 h light/dark cycle; lights on 8:00 PM) and temperature (21 ± 2 °C) controlled vivarium rooms. Food (Envigo Teklad 18% Protein Rodent Diet; #2018) and water were available ad libitum. All procedures involving the housing and use of experimental animals were approved by the Scripps Research Institutional Animal Care and Use Committee (IACUC; protocol no. 09–0004 and 09–0006) and in accordance with the National Institutes of Health Guide for the Care and Use of Laboratory Animals.

Experimental design

These experiments included 3 cohorts of mice: Cohort 1 (Astrocyte-TRAP mice; male $n = 15$; female $n = 17$), Cohort 2 (C57BL/6 J mice; male $n = 79$; female $n = 68$), and Cohort 3 (C57BL/6 J mice; male $n = 44$; female $n = 65$). Cohort 1 consisting of Astrocyte-TRAP mice underwent the CIE-2BC protocol and a subset (7 M/9F) were used for TRAP RNAseq and TRAP qRT-PCR experiments. Cohort 1 mice were euthanized after the 4th day of CIE during the 5th round. Cohort 2 consisting of C57BL/6 J mice underwent the CIE-2BC protocol and distinct subsets were used for RNAscope (8 M/8F), multiplex cytokine assays (16 M/30F), western blot experiments (25 M), and electrophysiological recordings (30 M/30F). For electrophysiological recordings, some mice were euthanized immediately after their last vapor session (Dep group) while others were euthanized after 4–7 full days of alcohol withdrawal (WD group). Cohort 3 consisting of C57BL/6 J mice underwent the CIE-2BC protocol with IL-6R Ab or IgG2b isotype control injections during the last round of CIE-2BC. Distinct subsets from Cohort 3 were used for multiplex cytokine assays (9 M) and electrophysiological recordings (3 M/6F). For all experiments, other than the electrophysiology recordings of the WD group, mice in Cohorts 2 and 3 were euthanized immediately after their last 16 h ethanol vapor session following the 4th – 5th round (Dep group) or when this session would have occurred (for time-matched naïve and Non-Dep groups). Experimental sample sizes were determined using power analyses based on prior studies where appropriate. Estrous cycles were not monitored to maintain sufficient power within current sample sizes.

Chronic intermittent ethanol vapor exposure—two-bottle choice (CIE-2BC)

The mouse CIE-2BC model of alcohol dependence-induced escalation of drinking was conducted as previously reported [48, 49, 51–54]. Briefly, the CIE-2BC paradigm produces three groups of mice differing in

their alcohol experience: 1) naïve mice with no exposure to alcohol (no EtOH, naïve); 2) alcohol experienced, not dependent, mice with a history of voluntary drinking but no ethanol vapor exposure (2BC only, Non-Dep); and 3) alcohol experienced, dependent mice that exhibit excessive and escalated alcohol intake after chronic ethanol vapor exposure (CIE-2BC, Dep).

First, to establish baseline (BL) drinking, 2BC testing was performed 5 days per week (M-F) for 2–4 consecutive weeks. Mice were singly housed 30 min before the lights went off and given 2 h access to two drinking tubes (15% w/v ethanol in tap water vs. tap water only). During this time, mice in the naïve group received 2 water bottles. After the completion of each 2 h 2BC drinking session, mice were returned to their group-housed home cages. Following this BL phase, alcohol drinking mice were divided into two groups (Non-Dep and Dep) with balanced alcohol and water consumption. Mice in the Dep group were injected intraperitoneally (*i.p.*) with 1.75 g/kg alcohol + 68.1 mg/kg pyrazole (alcohol dehydrogenase inhibitor) and placed in alcohol vapor chambers (La Jolla Alcohol Research, La Jolla, CA, USA) for 4 days (16 h vapor on, 8 h off). These alcohol + pyrazole injections prior to each vapor exposure stabilize blood alcohol levels (BALs) in the target range and decrease variability across exposure and between mice. BALs were determined immediately upon vapor chamber removal on the third day of exposure during every round via tail blood samples collected in heparinized capillary tubes and centrifuged for 20 min at 13,000 rpm at 4 °C. The supernatants were then processed on an Agilent 7820 A gas chromatograph coupled to a 7697 A headspace sampler. Alcohol drip rates were manipulated to maintain BALs that reliably produce dependence (150–200 mg/dL) [37, 48]. Mice in the Non-Dep group were injected with 68.1 mg/kg pyrazole, placed into identical caging, and exposed to air. Naïve mice were injected with 68.1 mg/kg pyrazole and returned to the home cage. Vapor/air exposure was followed by 72 h of abstinence and 5 days of 2BC testing. This regimen was repeated an additional three to four more times for a total of four or five full rounds. In Dep mice, euthanasia occurred immediately following the final alcohol vapor exposure (16 h) and tail blood was collected to determine terminal BALs. Euthanasia occurred in a time-matched manner for mice that were not exposed to ethanol vapor (Non-Dep and naïve).

Postmortem human brain RNA-seq

Complete methodological details are part of an already published study [59] and were performed as previously reported [60]. The RNA-seq data and sample details are available through the NCBI BioProject database (Central Nucleus Amygdala: PRJNA551908). Briefly, central nucleus of the amygdala samples (30 AUD [23 M/7F] and 30 matched controls [23 M/7F] over 18 years of age) were obtained from the New South Wales Tissue Resource Centre at the University of Sydney. RNA was extracted using the Qiagen RNeasy kit (Qiagen, Germantown, MD, USA). The RNA-seq samples were prepared using the TruSeq RNA Library Pre Kit v2 (Illumina, Inc., San Diego, CA, USA) and sequenced on the Illumina HiSeq 2000 at the Genome Sequencing and Analysis Facility (GSAF) at The University of Texas at Austin. Raw reads were aligned to human genome 38 (GRCh38) using STAR aligner version 2.5.3. Reads were counted with Python/htseq and imported to R/DESeq2 for differential expression analysis.

Astrocyte-TRAP CIE-2BC

The mice used in this study for astrocyte specific RNA-Seq, TRAP-seq and qRT-PCR have previously been described for nucleus accumbens wherein all relevant methods are detailed in full [53]. CeA data presented here are part of a larger TRAP-seq and RNA-seq data set [61]. The raw sequencing data and gene read count table are available at the National Center for Biotechnology Information Gene Expression Omnibus site (https://www.ncbi.nlm.nih.gov/geo/) under accession GSE325031. Briefly, adult hemizygous B6;FVB-Tg(Aldh1l1-EGFP/Rpl10a)JD130Htz/J mice (Astrocyte-TRAP; Cohort 1) underwent CIE-2BC exposure as detailed above to generate naïve (8 M/8F), Non-Dep (4 M/5F), and Dep (3 M/4F) mice. Mice were exposed to vapor/air for a final (5th) round of CIE and were euthanized within an hour of removal from the chambers for brain collection. Brains were flash frozen in isopentane chilled in a dry ice isopropanol slurry and stored at −80 °C until utilized.

Translating ribosome affinity purification (TRAP) and RNA isolation

The CeA was collected bilaterally from 300 µm sections of frozen whole brains from Bregma −0.94 mm to −2.18 mm using a 1.5 mm punch tool [62]. Astrocyte translating RNA was immunoprecipitated (IP) using the TRAP procedure as described previously [63] with anti-GFP antibodies (Memorial-Sloan Kettering Antibody and Bioresource Core Facility; HtzGFP-19C8 & HtzGFP-19F7) and protein A/G magnetic beads (Thermo Fisher, 88,803). RNA was isolated from the input and IP samples using Trizol (Thermo Fisher, Carlsbad, CA) and the Direct-Zol RNA MicroPrep Kit (Zymo Research, Orange, CA).

RNA-seq

RNA from TRAP and input samples were submitted to the OHSU Integrated Genomics Laboratory (IGL) for library preparation and sequencing [53]. Samples were profiled using the Agilent Tapestation 4200 and sequenced on a NovaSeq 6000 (Illumina). Raw

sequencing reads were aligned to the mouse reference genome from Ensembl (GRCm38) with STAR aligner v2.7.10b [64]. DESeq2 v1.26.0 [65] was used to perform differential analysis for each dataset with Sex and TRAP pass as covariates.

TRAP qRT-PCR

To follow up on the significantly enriched pathways and further investigate changes in IL-6 signaling in Dep vs Non-Dep mice, qRT-PCR was carried out on a subset of input and IP samples used for the RNA-Seq as previously described [63, 66]. Input and IP RNA qRT-PCR was conducted using the Luna Universal One-Step RT-qPCR Kit (NEB) on the CFX96 (Bio-Rad) thermocycler with normalization to total RNA using the Quant-it RiboGreen kit (ThermoFisher). Primer sequences for *Il6ra* (*Il6ra* Forward: 5'-AGCGACACTGGGGACTATTTA-3'; Reverse: 5'-ACAGCCTTCGTGGTTGGAG-3') and *Il6st* (*Il6st* Forward: 5'- CTTTGGGCAGATCGAGCAGAA-3'; Reverse: 5'- CCCTCATTCACAATGCAAGTCA-3') were downloaded from PrimerBank [67]. For comparison of IP to Input samples, results are expressed as $\log_2$(fold change [FC] mRNA expression of IP/Input). For evaluation of sex and dependence as factors within IP samples, results are expressed as fold change/female Non-Dep.

Data analysis: qRT-PCR results comparing IP to Input samples were analyzed using a mixed-effects model with fraction (Input vs IP) as a within subjects factor and sex (M vs F) as well as group (Dep vs Non-Dep) as between subjects factors. qRT-PCR analysis within IP samples was performed using two-way ANOVA with sex (M vs F) and group (Dep vs Non-Dep) as between subjects factors. One sample from the male Dep group was excluded from the *Il6st* analysis due to poor amplification specificity during melt-curve analysis.

Bioinformatic analysis

Ingenuity Pathway Analysis (IPA, Qiagen) was used to identify enriched canonical pathways. IPA Canonical pathway enrichment analysis produces *p*-values corresponding to the significance of the enrichment, enrichment ratio corresponding to the number of enriched genes in the analyzed dataset divided by the total number of genes in the pathway, and activation z-score which is a prediction of pathway activation or inhibition based on the direction of regulation of genes in the dataset and known relationships within the pathway.

RNAscope in situ hybridization

RNAscope was performed as previously reported [49, 68–75]. Briefly, a total of 16 mice (Cohort 2; $n = 4$ per sex and experimental group [Naïve/Dep]; 3–4 images for each mouse) were deeply anesthetized with 3–5% isoflurane and transcardially perfused with Z-fix for 5 min. Brains were removed and post-fixed in Z-fix for 24 h at 4 °C, cryoprotected in sterile 30% sucrose in PBS for 24–48 h at 4 °C, snap-frozen in isopentane, and stored at −80 °C until use. Brains were sliced on a cryostat in 20 µm thick sections, mounted on SuperFrost Plus slides (Fisher Scientific, catalog no. 1255015), and stored at −80 °C until further processing.

In situ hybridization (ISH) was performed using the RNAscope multiplex fluorescent detection kit (ACD, catalog no. 320850) following the manufacturer's protocol (ACD, catalog no. 320535). Slides were incubated with the following probes: *Il6* (ACD, catalog no. 315891; encoding interleukin-6), *Il6ra* (ACD, catalog no. 435921-C1; encoding interleukin-6 receptor subunit alpha), *Itgam* (ACD, catalog no. 311491; encoding integrin alpha M; microglial marker), *Gfap* (ACD, catalog no. 313211-C2; encoding glial fibrillary acidic protein; astrocytic marker), and *Rbfox3* (ACD, catalog no. 313311-C2; encoding RNA-binding protein Fox-1 homolog 3; neuronal marker) for 2 h at 40 °C. A negative control probe (ACD, catalog no. 320871) was run in tandem. Signals were amplified to detect RNA transcripts for a total of 90 min at 40 °C. Slides were then mounted with DAPI-containing Vectashield (Fisher Scientific, catalog no. NC9029229).

Imaging and analysis

Images were acquired using a Zeiss LSM 780 laser scanning confocal microscope (40X oil immersion, 1024 × 1024, tile scanning of CeA at approximately bregma − 1.46 mm, 5-µm z-stacks) and all microscope settings were held constant between the experiments during image acquisition. For each mouse, 3–4 images of the medial subdivision of the CeA were collected. Analysis and quantification were performed using CellProfiler [68–72, 76]. Nuclei were identified based on DAPI staining and considered positive for a given probe if the corresponding fluorescent signal exceeded background levels (negative control). The percentage of positive nuclei was calculated and normalized to the naïve group. To validate CellProfiler results, a random set of images were quantified manually in Fiji. Brightness, contrast, and pixel dilation were kept consistent across representative images. All analyses were performed on raw images.

Data analysis: Female and male samples were analyzed separately as they were processed and imaged separately. A data point was considered an outlier if it was identified as such by both ROUT (Q = 1%) and 1.5xIQR and removed accordingly. Normality and homogeneity of variance were assessed using the Shapiro–Wilk and F tests, respectively. Data that were not normally distributed were analyzed with the Mann–Whitney test. All other data were analyzed using unpaired, two-tailed,

t-tests and Welch's correction was applied when the assumption of equal variances was violated.

Multiplex assay of central amygdala cytokine levels

To assess cytokine levels in the CeA, a total of 55 mice consisting of subsets from Cohort 2 (16 M/30F) and Cohort 3 (9 M) were analyzed. Specifically, samples included naïve (8 M/8F), Non-Dep (9 M/10F), and Dep (8 M/12F) groups. First, mice were anesthetized with 3–5% isoflurane, transcardially perfused with phosphate-buffered saline, and decapitated. Brains were rapidly removed, snap-frozen in isopentane, and stored at −80 °C until use. Brains were sliced on a cryostat in 18 µm thick sections. The CeA was isolated using 0.8 mm punches and stored at −80 °C until further processing. Samples were homogenized using 80 µL of 25 mg/mL AEBSF (ThermoFisher Scientific, Catalog No. 78431) in homogenization buffer consisting of 0.02 M Tris HCl (pH 7.5), 0.15 M NaCl, and 0.05% (v/v) Tween 20 in H_2O. Homogenate was placed on ice for 10 min and then centrifuged at 14,000 g for 10 min at 4 °C. Supernatant was collected and total protein concentration was measured using the Bio-Rad DC protein assay (Bio-Rad, Hercules, CA, USA). Samples were aliquoted and stored at −80 °C until use. Cytokine levels were tested in duplicate using a Mouse Cytokine/Chemokine Magnetic Bead Panel kit that included 8 of the 32 preset analyte options: IL-6, interleukin-1β (IL-1β), interleukin-1α (IL-1α), interferon-γ (IFN-γ), tumor necrosis factor-α (TNF-α), interleukin-10 (IL-10), interleukin-17 (IL-17), and monocyte chemoattractant protein-1 (MCP-1), (MCYTOMAG-70 K; MilliporeSigma, Burlington, MA, Kit lot # 4,150,931) using the manufacturer's protocol on a Luminex xMAP system with xPONENT software (Luminex Corporation, Austin, TX), as previously reported [49, 77–79]. One Non-Dep female sample was excluded prior to the DC protein assay due to insufficient tissue collection and one naïve female sample was excluded from the Luminex assay due to an error during plate preparation. Intra-assay coefficients of variation were < 10%.

Data analysis

Female and male samples were analyzed separately as they were run on different assay plates. A data point was considered an outlier if it was identified as such by both ROUT (Q = 1%) and 1.5xIQR and removed accordingly. Normality and homogeneity of variance were assessed using the Shapiro–Wilk and Brown-Forsythe tests, respectively. Data that were not normally distributed were analyzed with the Kruskal–Wallis test and Dunn's post hoc test. Welch's ANOVA with Dunnett's T3 post hoc test was used when the assumption of equal variances was violated. All other data were analyzed using ordinary one-way ANOVA followed by Tukey's post hoc test.

Western blot

Western blot analyses for brain regional changes in protein were conducted in mice as previously described [37, 50, 80]. Alcohol Dep (n = 12 M) and Non-Dep (n = 13 M) mice from Cohort 2 were anesthetized with 3–5% isoflurane, decapitated, and brains were rapidly removed, snap-frozen in isopentane, and stored at −80 °C. Twelve to twenty-four hours before dissection, brains were moved to −20 °C. Brains were then mounted and sliced using a cryostat at −12 °C, central amygdala brain punches (0.5 mm thick) were obtained using a 16 gauge needle according to the mouse brain atlas [62]. Brain punches were homogenized by sonication in a lysis buffer (in (mM): 320 sucrose, 5 HEPES, 1 EGTA, 1 EDTA, 1% SDS), protease inhibitor cocktail (diluted 1:100), and phosphatase inhibitor cocktails II and III (diluted 1:100) (Sigma, St. Louis, MO, USA). Tissue homogenates were heated at 95 °C for 5 min and the total protein concentration was measured using a detergent-compatible Lowry method (Bio-Rad, Hercules, CA, USA). The samples were aliquoted and stored at −80 °C until use. Protein samples (20 µg) were separated by SDS–polyacrylamide gel electrophoresis on 8–12% acrylamide gels using a Tris/Tricine/SDS buffer system (Bio-Rad). The gels were electrophoretically transferred to polyvinylidene difluoride membranes (GE Healthcare, Piscataway, NJ, USA). Membranes were blocked for 1 h in 5% non-fat milk at room temperature and incubated overnight in 2.5% non-fat milk with primary antibody at 4 °C. The primary antibodies included were $pSTAT3^{Y705}$ (1:10,000; Cell Signaling; Cat #9145), GP130 (1:5,000; Cell Signaling; Cat #3732), and SOCS3 (1:5,000, Abcam, Cat #16,030). Membranes were washed and incubated with species-specific peroxidase-conjugated secondary antibodies (1:10,000–1:20,000; Bio-Rad) for 1 h at room temperature. Membranes were washed and incubated in a chemiluminescent reagent (Immobilon Crescendo Western HRP Substrate, Millipore Corporation, Billerica, MA, USA) and exposed to film. Following film development, membranes were stripped for 30 m at room temperature (Restore; Thermo Scientific) and re-probed for either total STAT3 (1:10,000; Cell Signaling; Cat #9139) or β-tubulin (1:1,000,000; Santa Cruz Biotechnology; Cat # 05–797R) levels. The immunoreactivity of the bands was detected using densitometry (Image J 1.45S; Bethesda, MD). To normalize the data across the blots, the densitometric values were expressed as a percentage of the mean of the naïve controls for each gel. Individual mouse GP130, and SOCS3 levels were normalized to individual β-tubulin protein levels and pSTAT3 levels were normalized to total STAT3 levels to generate ratio values for statistical comparison.

Data analysis

Normality and homogeneity of variance were assessed using Shapiro–Wilk and F tests, respectively. Data that were not normally distributed were analyzed with the Mann–Whitney test. All other data were analyzed using unpaired, two-tailed, t-tests.

Electrophysiology and GABAergic transmission

Ex vivo whole-cell patch-clamp electrophysiology recordings [37, 48, 50] were carried out in CeA neurons of mice from Cohorts 2 (30 M/30F) and 3 (3 M/6F) divided into naïve (13 M/12F), Non-Dep (6 M/7F), Dep (7 M/10F) and WD (7 M/7F) groups. Neurons were visualized under infrared differential interference contrast (IR-DIC) microscope and synaptic currents were recorded with borosilicate glass capillaries (2–5 mΩ) filled with the KCl-based internal solution (in mM: 135 KCl, 10 HEPES, 2 $MgCl_2$, 5 EGTA, 2 Mg-ATP, and 0.2 Na-GTP, 290–310 mOsm, pH adjusted to 7.2–7.4 using 1 M KOH). The CeA neurons were held at −60 mV. The $GABA_A$ receptor-mediated spontaneous inhibitory postsynaptic currents (s/mIPSCs) were pharmacologically isolated by slice perfusion (> 10 min) in artificial cerebrospinal fluid (aCSF) containing AMPA and NMDA receptor antagonists DNQX and DL-APV (20 μM and 30 μM, respectively, Tocris, Minneapolis, MN) and $GABA_B$ receptor antagonist CGP55845A (1 μM, Tocris), and tetrodotoxin (0.5 μM), in the case of mIPSCs [37]. We recorded in a gap-free mode before (baseline) and during application (for 15 min) of the recombinant murine IL-6 (50 ng/ml; PeproTech, Cranbury, NJ; Catalog # AF-216–16-50UG). Data acquisition was done with Multiclamp 700B amplifier, 1440 Digitizer, and Clampfit 10 software (Molecular Devices, Sunnyvale, CA). GABAergic sIPSCs were analyzed with MiniAnalysis version 6.0.8 (provided by BlueCell, Seoul, South Korea). Cells with more than 20% change in access resistance (Ra ≤ 15 MΩ, monitored with frequent 10 mV pulses) were excluded from the final data analysis. We analyzed sIPSC frequencies, amplitudes, kinetics (rise and decay times) followed by a visual inspection of each individual event. The maximum IL-6 effect was calculated from 3-min bins between 6 and 15 min after IL-6 application and used for statistical analyses.

Data analysis

Regarding figures in the main text of this paper, if the data had equal variance and were normal according to the Kolmogorov–Smirnov test, final values were analyzed using one-sample t-tests. If the data were nonparametric, a one sample Wilcoxon test was used. Regarding additional electrophysiological figures in the supplementary materials, comparisons among three or more groups were analyzed using a one-way ANOVA when data met assumptions of normality and equal variance, a Welch's ANOVA when normality was met but variances were unequal, or a Kruskal–Wallis test when data were nonparametric. Comparisons with two or less groups were analyzed using unpaired, two-tailed student's t tests when data were normally distributed and exhibited equal variances. When data were better described by a lognormal distribution and/or variances were unequal, a lognormal Welch's t test was used.

IL-6R Ab injections during CIE-2BC

Adult C57 BL/6 J mice (Cohort 3; 44 M/65F) underwent CIE-2BC exposure as detailed above to generate Non-Dep (IgG2b: 12 M/15F; IL-6R Ab: 12 M/16F) and Dep (IgG2b: 9 M/16F; IL-6R Ab 11 M/18F) mice. A subset of these mice was included in a recently published study of IL-6R Ab's effect on alcohol-associated pain sensitivity [49]. In these, starting 24 h after the last vapor/air exposure session in the 4th – 5th round, IL-6R Ab or the isotype control IgG2b were injected *i.p.* (150 μg/day) daily, 30 min prior to the 2BC session (or the time when the 2BC session would have occurred for injections during withdrawal) for 7 days. Thus, the first two injections occurred during withdrawal while the five remaining injections occurred on the 5 days of 2BC. Dep mice whose drinking did not escalate by the final vapor exposure session were excluded from the study (4 M/9F). Before euthanasia, mice were exposed to a single air/alcohol vapor exposure (Non-Dep and Dep, respectively; 16 h) and tail blood was collected to determine terminal BALs.

Data analysis

Alcohol and water intake (g/kg) were analyzed using two-way repeated measures (within [time] – between [experimental group]) ANOVA and the Geisser-Greenhouse correction. On one day, the water bottle of a Non-Dep female in the IL-6R Ab treated group leaked resulting in a missing value, a mixed-effects model (REML) was used to analyze water intake for the Non-Dep females accordingly. Average weekly alcohol intake (g/kg) was analyzed using one-way repeated measures (within [time]) ANOVA and the Geisser-Greenhouse correction followed by Dunnet's post hoc test.

Drugs

For behavioral experiments, anti-mouse IL-6R antibody (BioXCell, Catalog# BE0047, Clone 15A7, Lot #795921D1) or isotype control rat IgG2b antibody (BioXCell, Catalog# BE0090, Clone LTF-2, Lot #767921D1) were prepared fresh in dilution buffer (BioXCell, Catalog# IP0700, Lot #762122D1) on each injection day to a concentration of 750 μg/mL and administered at 150 μg/200 μL intraperitoneally (*i.p.*) [49]. The IL-6R Ab dose

and frequency of administration were consistent with prior work [29]. Additionally, the *i.p.* route of administration has been previously employed to examine the effects of IL-6R Ab in preclinical models of central nervous system (CNS)-related disorders which suggests an effect in the CNS [29, 49, 81–88]. Alcohol for 2BC drinking sessions was prepared as 15% ethanol (w/v, ethanol in tap water). Pyrazole (Sigma, St. Louis, MO) was dissolved in saline for *i.p.* injections during the CIE-2BC protocol.

Statistical analysis

Experimental group sizes (n) used for each experiment are described in the corresponding methods section as well as figure legends. Statistical analyses performed for each experiment are described in detail in the corresponding methods section. All data were analyzed and graphed using GraphPad Prism 10 software (La Jolla, California) unless otherwise stated in the corresponding methods section. Statistical significance was defined a priori as $p < 0.05$ unless otherwise stated in the corresponding methods section. See Supplemental Table S5 for all statistical tests and factors. In addition, see Supplemental Table S6 for statistical details of supplemental figures.

Results

Immune-related genes, including IL-6, are dysregulated in the human central amygdala in AUD

We first examined the translational validity of our hypothesis that chronic alcohol consumption activates neuroimmune signaling in the brain by utilizing RNA-sequencing on human postmortem CeA tissue samples from human donors with AUD as well as controls without AUD, the primary analysis of which has been published in full [59]. We identified 377 differentially expressed genes (DEGs) with $|\log_2[FC]| > 0.15$ and nominal p-values ≤ 0.01. Of these, 204 genes were upregulated and 173 were downregulated, indicating significant molecular alterations in AUD. Pathway enrichment analysis using clusterProfiler (v4.4.4) revealed robust enrichment in immune response (GO:0006955, $p = 1.7e\text{-}8$) and extracellular matrix organization (GO:0030198, $p = 5.2e\text{-}5$), suggesting neuroinflammation and structural remodeling in AUD pathology.

The pro-inflammatory cytokine *IL6* exhibited significant upregulation in individuals with AUD compared to controls ($|\log2[FC]| = 2.1803$, $p = 1.3e\text{-}4$; Fig. 2), highlighting its role in neuroinflammatory processes. Other immune-related genes showed notable changes, including suppressor of cytokine signaling 3 (*SOCS3*; $|\log_2[FC]| = 1.76$, $p = 1.0e\text{-}4$), leukemia inhibitory factor (*LIF*; $|\log_2[FC]| = 2.9967$, $p = 4.2e\text{-}6$), C–C motif chemokine ligand 2 (*CCL2*; $|\log_2[FC]| = 1.6159$, $p = 1.6e\text{-}5$), platelet factor 4 (*PF4*; $|\log_2[FC]| = 2.1654$, $p = 3.4e\text{-}3$), tumor necrosis factor receptor superfamily member 12 A (*TNFRSF12A*; $|\log_2[FC]| = 1.3208$, $p = 1.3e\text{-}3$), FOS-like antigen 1 (*FOSL1*; $|\log_2[FC]| = 2.2461$, $p = 2.1e\text{-}4$), and retinoic acid early transcript 1L (*RAET1L*; $|\log_2[FC]| = 2.4435$, $p = 1.6e\text{-}3$) reinforcing a strong inflammatory signature. Conversely, major histocompatibility complex, class I, A (*HLA-A*) was significantly downregulated ($|\log_2[FC]| = -1.5346$, $p = 1.3e\text{-}3$), suggesting impaired antigen presentation and compromised immune recognition. Additional immune-related genes, such as antigen-presenting glycoprotein CD1d (*CD1D*; $|\log_2[FC]| = 0.8028$, $p = 5.5e\text{-}3$) and *IL1B* ($|\log_2[FC]| = 1.1325$, $p = 3.0e\text{-}3$) were upregulated, further supporting immune response dysregulation. Further, immune response-related genes such as 14–3-3 protein sigma (*SFN*; $|\log_2[FC]| = 2.5271$, $p = 7.0e\text{-}4$) were upregulated, indicating broad stress and inflammatory responses. These results emphasize the critical role of immune response dysregulation, particularly through *IL6* signaling and associated pathways, in AUD. Differential expression analysis results of IL6 signaling pathway genes in human postmortem CeA samples from donors with AUD as compared to controls are presented in Supplemental Table S1.

The IL-6 signaling pathway is differentially regulated in central amygdala astrocytes in the context of alcohol dependence

Astrocytes and microglia are the main components of the brain innate immune system. While under physiological conditions, astrocytes play a homeostatic role essential to proper function of the brain while under pathological conditions, they can become reactive and express and release neuroimmune factors including IL-6 [89, 90]. We have reported that the CIE-2BC protocol induces astrocyte reactivity in the NAc and CeA [53, 61]. The human central amygdala transcriptomic data in the previous section, and preclinical evidence suggest that astrocyte specific production of IL-6 contributes to decreased stress-coping behaviors [47] and increased alcohol withdrawal susceptibility [46]. Based on this, we used Aldh1l1-EGFP/RPL10a (astrocyte TRAP) mice which express an EGFP tagged ribosomal protein Rpl10a in astrocytes allowing for the pull-down of astrocyte specific RNA using the TRAP procedure [53]. Paired with the CIE-2BC paradigm, these mice facilitated determination of the astrocyte specific contribution to increased IL-6 signaling in the context of alcohol dependence.

Ingenuity Pathway Analysis (IPA) of the "IL-6 signaling" canonical pathway of CeA astrocyte-specific TRAP-isolated translating mRNAs revealed limited "IL-6 signaling" pathway engagement in Non-Dep vs naïve mice (2 differentially regulated genes; Table S2), but substantially broader "IL-6 signaling" pathway dysregulation

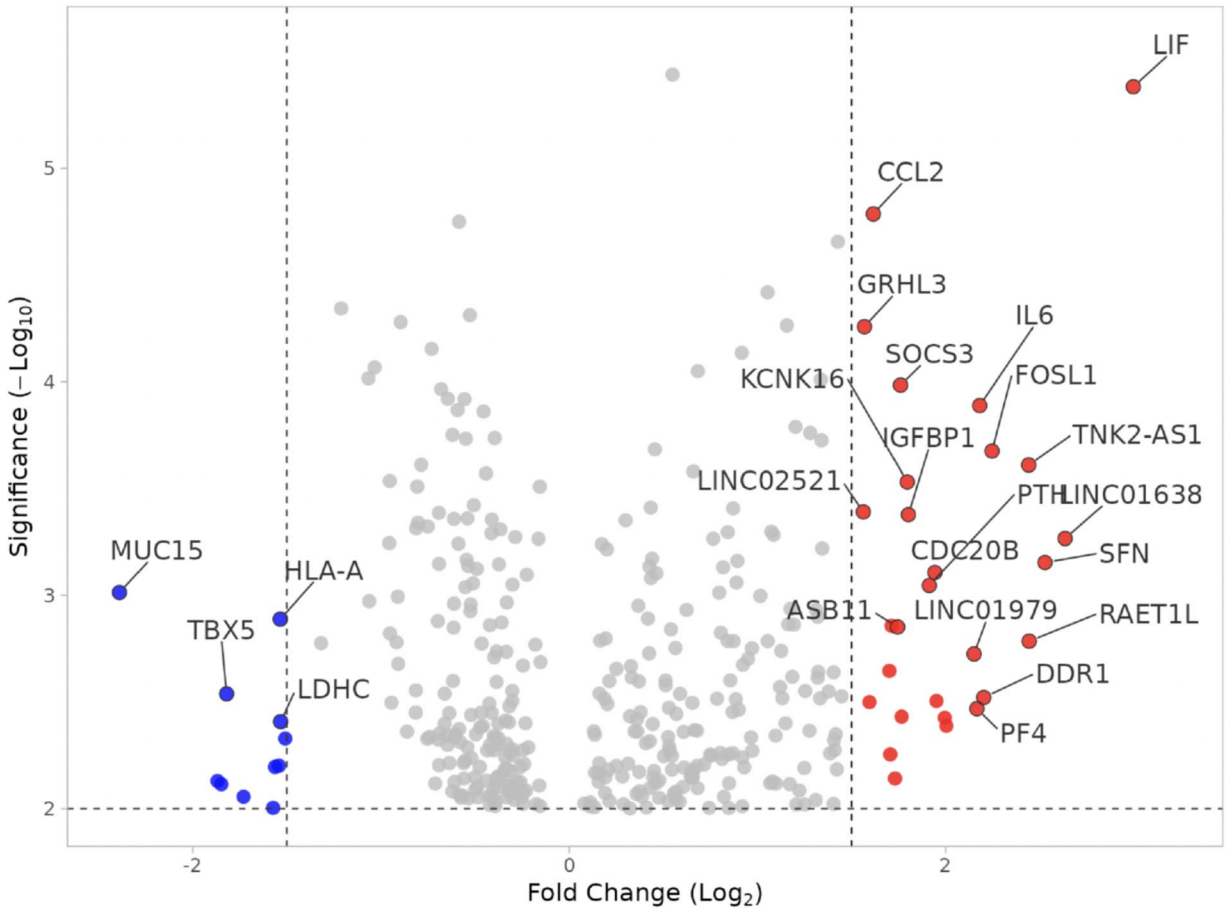

Fig. 2 Immune-related genes, including IL-6, are dysregulated in the human central amygdala in AUD. The volcano plot shows differential gene expression between the control and AUD groups ($n = 30$ per group; 23 males and 7 females). Each point represents a gene, with the x-axis showing log2 fold change (log_2[FC]) and the y-axis showing the negative logarithm (base 10) of the unadjusted p-value (-log_{10}[p-value]). Genes with |log_2[FC]|> 1.5 and nominal *p*-value ≤ 0.01 are plotted in color, with upregulated genes shown in red and downregulated genes shown in blue. Vertical and horizontal dashed lines indicate the fold change and significance cutoffs, respectively

in Dep vs naïve mice (10 differentially regulated genes; Table S3). A direct comparison of Dep vs Non-Dep mice further identified 7 differentially regulated genes in the "IL-6 signaling" pathway (Table S4), suggesting progressive astrocytic IL-6 signaling alterations with the transition to dependence. Of note, differentially regulated genes in Dep mice compared to Non-Dep mice included suppressor of cytokine signaling 1 (*Socs1*), *Stat3*, tumor necrosis and factor receptor superfamily member 1a (*Tnfrsd1a*), as well as phosphatidylinositol-4-phosphate 3-kinase catalytic- and phosphoinositide-3-kinase regulatory-subunits (*Pik3c*[s] and *Pik3r*[s]), consistent with dysregulation of members of TNF receptor family and Pik3C subunits, and trend for upregulation of STAT3 in human postmortem CeA samples from donors with AUD as compared to controls (Table S1). Thus, "IL-6 signaling" was identified as a significantly enriched IPA canonical pathway, when comparing Dep vs Non-Dep mice (Fig. 3A). Specifically, 7 of the 109 genes in this pathway were differentially regulated (Table S4) and the activation z-score was 1.13, which suggests predicted activation of the overall pathway based on known relationships within the pathway. This includes predicted upregulation of *Il6* and *Socs3*, consistent with their observed upregulation in the CeA of human donors with AUD (Fig. 2), as well as predicted downregulation of Janus kinase 2 (*Jak2*), however we did not directly observe these patterns of regulation in the RNA-Seq data. These findings indicate that the IL-6 signaling pathway is regulated selectively during the process of developing alcohol dependence, therefore, in the remainder of this report, we prioritize study of the Dep condition.

To follow up on the significantly enriched pathway and further investigate changes in IL-6 signaling in Non-Dep vs Dep mice, TRAP qRT-PCR analysis was conducted on *Il6st* (gp130) and *Il6ra*, representing genes encoding the subunits of the IL-6 receptor. *Il6ra* showed significantly less expression in the astrocyte fraction compared to the

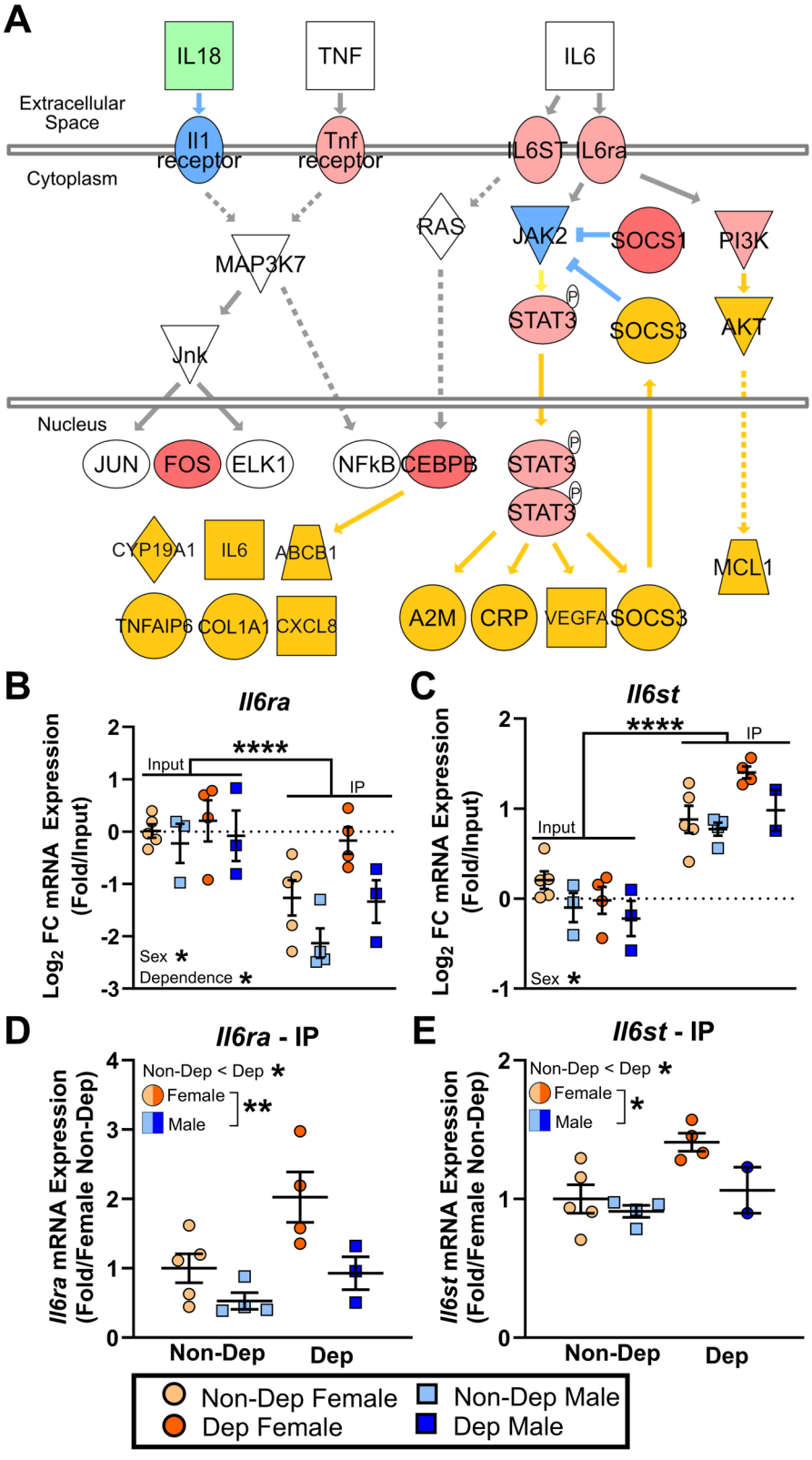

Fig. 3 (See legend on next page.)

(See figure on previous page.)

Fig. 3 The IL-6 signaling pathway is differentially regulated in central amygdala astrocytes in the context of alcohol dependence. **A** IL-6 signaling pathway denoting the differential gene expression identified by TRAP-seq analysis (modified from IPA schematic). Genes upregulated in the Dep condition are shown in pink or red (with greater log_2[fold change] in red), while downregulated genes are shown in green. Genes with predicted upregulation and downregulation in the Dep condition are shown in yellow and blue, respectively. Dashed lines indicate simplification of the signaling pathway with unchanged proteins removed for simplicity. *Il6st* and *Il6ra* expression levels are based on TRAP qRT-PCR results. **B-E** TRAP qRT-PCR of *Il6ra* (**B**&**D**) and *Il6st* (**C**&**E**) in bulk-tissue (Input) and astrocyte translating RNA (immunoprecipitated, IP) from male ($n = 7$; blue squares) and female ($n = 9$; orange circles), and Dep (dark shade) and Non-Dep (light shade) mice. **B**&**C** mRNA expression of *Il6ra* and *Il6st* in IP as compared to Input samples. Results are expressed as log_2(fold change [FC] mRNA expression of IP/Input) and analyzed using three-way ANOVA. **D**&**E** *Il6ra* and *Il6st* mRNA levels in IP samples only. Results are expressed as mean ± SEM and analyzed using two-way ANOVA. Significant differences are denoted by $^*p < 0.05$, $^{**}p < 0.01$ and $^{****}p < 0.0001$. See Table S5 in Supplemental Materials for statistics relevant to each panel

bulk CeA RNA (Fig. 3B; $F_{1,23} = 26.4$, $p < 0.0001$), while *Il6st* showed robust enrichment in the astrocyte fraction (Fig. 3C; $F_{1,22} = 108.4$, $p < 0.0001$). In addition, *Il6st* showed ~ 14-fold higher expression in the CeA than *Il6ra* (data not shown). TRAP qRT-PCR of *Il6ra* revealed a significant main effect of dependence in CeA astrocytes with an increase of *Il6ra* in Dep mice when compared to Non-Dep controls (Fig. 3D; $F_{1,12} = 7.9$, $p = 0.02$). There was also a main effect of sex with increased expression of *Il6ra* in females as compared to males (Fig. 3D; $F_{1,12} = 9.6$, $p = 0.009$). Similarly, there were significant main effects of dependence and sex on *Il6st* in CeA astrocytes with increased *Il6ra* in the Dep when compared to the Non-Dep condition as well as female mice when compared to males (Fig. 3E; Dependence: $F_{1,11} = 8.6$, $p = 0.01$; Sex: $F_{1,11} = 5.1$, $p = 0.04$). Taken together, these results demonstrate that alcohol dependence alters the IL-6 signaling pathway.

Alcohol dependence induces cell-type and sex-specific changes in *Il6* expression in central amygdala astrocytes, neurons, and microglia

To further investigate the cellular distribution of *Il6* and its receptor *Il6ra* across distinct brain cell populations (astrocytes, neurons, and microglia), we performed RNAscope in situ hybridization (ISH) focusing on alcohol naïve and Dep mice (Fig. 4). Representative RNAscope images are shown in Fig. 4A and B for males and females, respectively, while the negative control image is shown in supplemental Figure S1. In alcohol Dep male mice, *Il6* colocalization with the astrocytic marker, *Gfap*, was similar to naïve controls (Fig. 4C). However, there was significantly increased colocalization of *Il6* with the neuronal marker, *Rbfox3* (Fig. 4D; Mann–Whitney U Statistic = 32, $p = 0.02$), as well as the microglial marker, *Itgam* (Fig. 4E; $t = 2.2$, $df = 18$, $p = 0.045$), in Dep male mice when compared to naïve controls. Similarly, in Dep females there was significantly increased colocalization of *Il6* with *Itgam* (Fig. 4H; $t = 2.3$, $df = 18.2$, $p = 0.03$), but not *Gfap* (Fig. 4F) or *Rbfox3* (Fig. 4G). In contrast, there were no significant changes in colocalization of *Il6ra* with astrocytes (Fig. 4I), neurons (Fig. 4J) or microglia (Fig. 4K) in Dep males. Meanwhile, there was a decrease in colocalization of *Il6ra* with the astrocytic marker, *Gfap* (Fig. 4L; $t = 3.0$, $df = 26$, $p = 0.006$), but not neurons (Fig. 4M) or microglia (Fig. 4N) in Dep females compared to naïve controls. Meanwhile, there was no change in the percentage of *Il6*$^+$, *Il6ra*$^+$, *Gfap*$^+$, *Rbfox3*$^+$, or *Itgam*$^+$ cells in Dep males or females when compared to naïve controls, except for an increase in *Rbfox3*$^+$ cells in Dep males (Fig. S2; $t = 2.1$, $df = 27$, $p = 0.04$). Overall, these results indicate that alcohol dependence modulates IL-6 signaling in a cell-type and sex-specific manner, increasing *Il6* mRNA co-localization microglia in both sexes and neurons in males, while only altering *Il6ra* expression in astrocytes of Dep females.

Alcohol dependence increases IL-6 in females and activates the STAT3 signaling pathway in the central amygdala in males

To further characterize the effects of CIE-2BC on IL-6 and other inflammatory targets, we determined their protein abundance in the CeA of naïve, Non-Dep, and Dep male and female mice using a multiplex assay with the Luminex xMAP system (Fig. 5). There were no significant differences in IL-6 levels in relation to alcohol exposure in males (Fig. 5A). IL-1β was significantly increased in Dep males when compared to their Non-Dep counterparts (Fig. 5B; $H_2 = 7.6$, $p = 0.02$), but no significant differences were detected in IL-1α, IFN-γ, or TNF-α (Fig. 5C-E). In contrast to males, CIE-2BC more broadly altered immune activation in the CeA of Dep females. Specifically, elevated levels of IL-6 were observed in Dep females when compared to their naïve and Non-Dep counterparts (Fig. 5F; $F_{2,25} = 8.9$, $p = 0.001$). In addition, alcohol dependence increased IL-1β and IL-1α in female mice when compared to naïve and Non-Dep groups (Fig. 5G & H; IL-1β: $W_{2.0,15.5} = 12.6$, $p = 0.0006$; IL-1α: $W_{2.0,15.4} = 13.7$, $p = 0.0004$). Finally, alcohol dependence increased IFN-γ and TNF-α in female mice when compared to their Non-Dep counterparts (Fig. 5I & J; IFN-γ: $F_{2,23} = 6.9$, $p = 0.004$; TNF-α: $F_{2,24} = 5.7$, $p = 0.01$). No significant differences were observed in IL-10, IL-17, or MCP-1 levels (Figure S3).

Luminex assay indicated that there was a main effect of alcohol exposure on IL-6 protein abundance in the CeA of female but not male mice. Thus, we used western blotting (WB) to further examine potential downstream

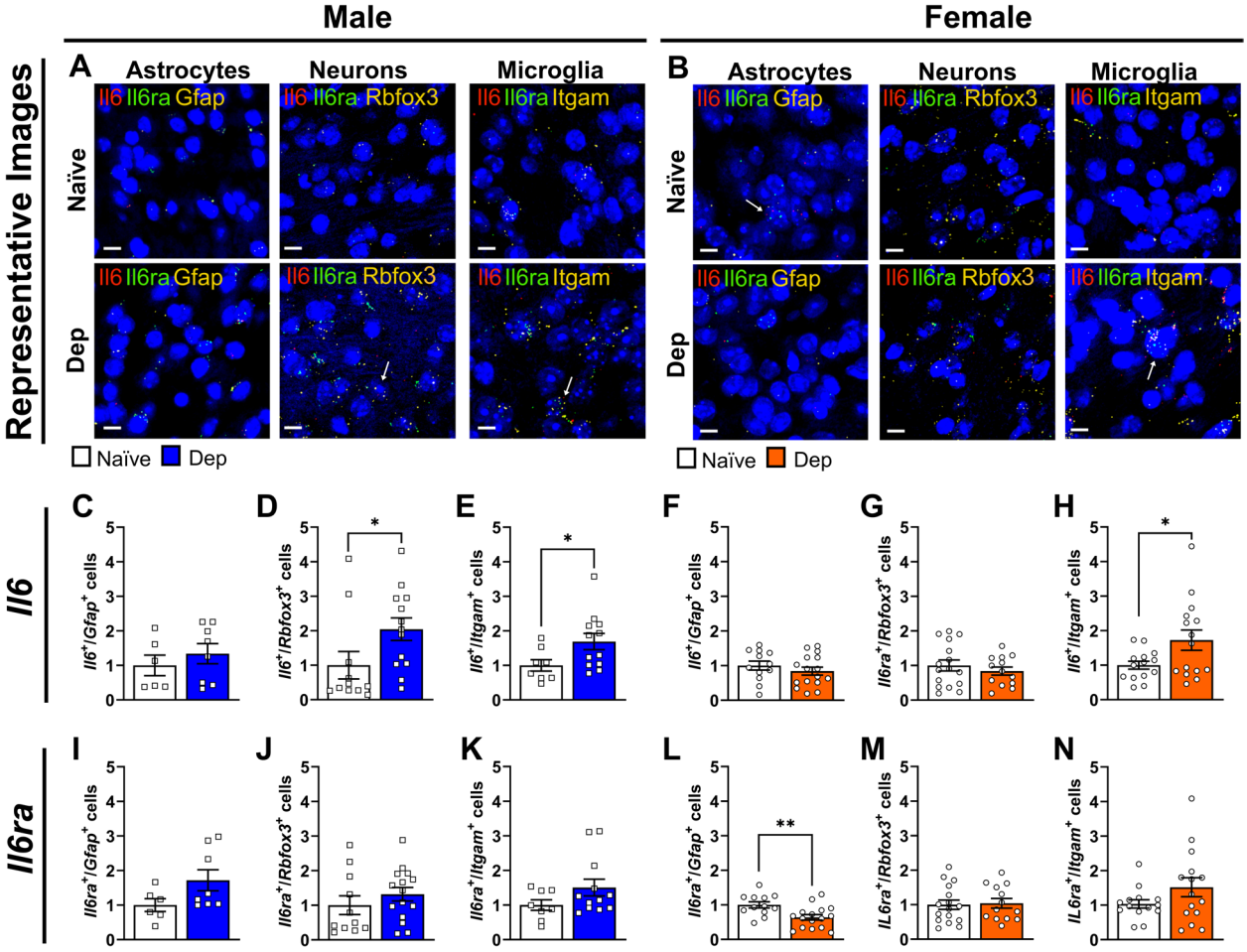

Fig. 4 Alcohol dependence induces cell-type and sex-specific changes in *Il6* expression in central amygdala astrocytes, neurons, and microglia. **A**-**B** Representative images from the medial subdivision of the CeA in male (**A**) and female (**B**) mice showing *Il6* (IL-6, red) and *Il6ra* (IL-6R, green) mRNA expression assessed by RNAscope/ISH ($n = 3$–4 per sex and experimental group; 3–4 images for each mouse), also see Fig. S1. Co-localization is shown with *Gfap* (GFAP, yellow), *Rbfox3* (NeuN; yellow), *Itgam* (CD11b, yellow) and DAPI (blue), labeling putative astrocytes, neurons, and microglia, respectively. Scale bar = 10 µm. White arrows indicate significant differences in co-localization. **C**-**N** Quantification (ratio) shows the normalized percentage of *Il6*$^+$ nuclei co-labeled with *Gfap*, *Rbfox3,* or *Itgam* (**C**-**H**) and the normalized percentage of *Il6ra*$^+$ nuclei co-labeled with *Gfap*, *Rbfox3,* or *Itgam* (**I**-**N**) in male (**C**-**E** & **I**-**K**; blue) and female (**F**–**H** & **L**-**N**; orange), naïve (white bars), and Dep (shaded bars) mice, relative to the percentage in naïve mice. Results are expressed as mean ± SEM and analyzed using unpaired, two-tailed t-test (**C**, **E–G**, **L**, **M**) with Welch's correction (**H**, **N**), as appropriate, or two-tailed Mann–Whitney test (**D**, **I-K**). Significant differences are denoted by $^*p < 0.05$. See Table S5 in Supplemental Materials for statistics relevant to each panel

changes in IL-6 signaling pathway activation in the CeA of male mice. Protein levels of phosphorylated STAT3 (pSTAT3), GP130, and SOCS3 were measured. We found that the phosphorylation of STAT3 at tyrosine 705 (indicative of STAT3 activation in terms of dimerization, nuclear translocation, and DNA binding) was significantly increased in the central amygdala of alcohol-dependent mice (Fig. 5K & L; Mann–Whitney U Statistic = 22, $p = 0.002$). No changes in GP130 (IL-6 receptor subunit) or SOCS3 (downstream negative regulator of IL-6 signaling) were observed between groups (Fig. 5M & N). These results indicate that alcohol dependence may activate central amygdala IL-6 signaling via the STAT3 pathway and by blocking the homeostatic potentiation of SOCS3 as a negative regulator of IL-6 signaling. Overall, our ISH, astrocyte-TRAP, Luminex, and WB data support dependence-induced upregulation of IL-6 signaling at both gene and protein levels.

IL-6 modulates CeA GABAergic transmission in a CIE-2BC treatment and sex-dependent manner

The CeA is mainly comprised of GABAergic neurons [7, 8]. Thus, to investigate the functional role of upregulated, pro-inflammatory IL-6 activity on CeA activity, we used whole-cell patch clamp electrophysiology to record pharmacologically isolated $GABA_A$ receptor-mediated synaptic currents in CeA neurons of alcohol naïve, Non-Dep, and Dep male and female mice. In addition, to assess the persistence of the effects of CIE-2BC on IL-6 modulation of GABAergic transmission, Dep mice were

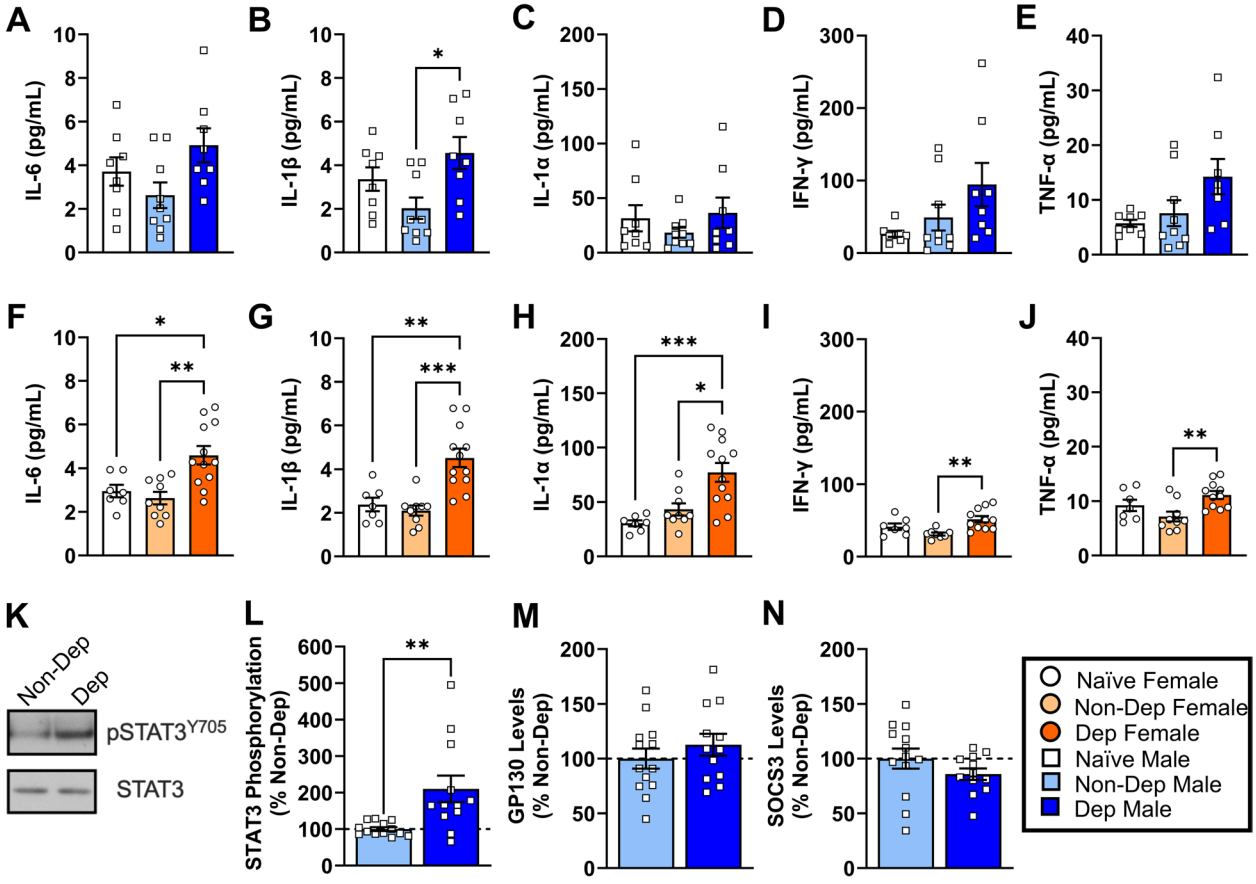

Fig. 5 Alcohol dependence increases IL-6 in females and activates the STAT3 signaling pathway in the central amygdala in males. **A**-**J** Multiplex assay cytokine levels (pg/mL) in the CeA of male ($n = 25$; **A**-**E**) and female ($n = 30$; **F**- **J**) mice after the CIE-2BC procedure: IL-6 (**A** & **F**); IL-1β (**B** & **G**); IL-1α (**C** & **H**); IFN-γ (**D** & **I**); TNF-α (**E** & **J**). **K**-**N** STAT3 signaling in the CeA of Dep and Non-Dep male mice. **K**. Representative images of the western blotting for phosphorylated STAT3 (pSTAT3^{Y705}) and total STAT3. **L**-**N** Bar graphs represent normalized OD values from Dep vs Non-Dep male mice ($n = 25$) for STAT3 phosphorylation (**L**), GP130 (**M**), and SOCS3 (**N**). Results are expressed as mean ± SEM and analyzed using one-way ANOVA (**A**, **F**, **I**, **J**), Welch's ANOVA (**G**, **H**) or the Kruskal–Wallis test (**B**-**E**) for multiplex assays and unpaired, two-tailed t test (**M**, **N**) or two-tailed Mann–Whitney test (**L**) for western blotting. Significant differences are denoted by $^{*}p < 0.05$, $^{**}p < 0.01$ and $^{***}p < 0.001$. See Table S5 in Supplemental Materials for statistics relevant to each panel

withdrawn (WD) from alcohol for 4–7 days prior to slice electrophysiology to form a fourth treatment group [80, 91, 92]. We recorded spontaneous inhibitory postsynaptic currents (sIPSCs) in CeA neurons before and during acute bath application of 50 ng/ml IL-6 for 15 min [93]. While there was a baseline difference (significant reduction) in sIPSC amplitude observed between naïve and WD males, we did not detect any significant differences in the remaining baseline sIPSC parameters of either sex or treatment group (Fig. S4).

Exogenous IL-6 significantly decreased the mean sIPSC frequency in Dep and WD male mice but did not alter the frequency in naïve and Non-Dep male mice (Fig. 6A & B). Specifically, IL-6 decreased sIPSC frequency to 72.5 ± 3.3% (one sample t-test, $p < 0.0001$) in Dep males and to 64.3 ± 6.9% (one sample t-test, $p = 0.0004$) in WD males. (Fig. 6B1). In Dep males, IL-6 significantly decreased sIPSC amplitude to 88.0 ± 5.3% (one sample t-test, $p = 0.043$) (Fig. 6B2). In naïve and WD males, IL-6 significantly increased rise time. Specifically, IL-6 increased sIPSC rise time to 109.3 ± 3.0% (one sample t-test, $p = 0.0015$) in naïve males and 115.3 ± 5.3% (one sample t-test, $p = 0.019$) in WD males (Fig. 6B3). Lastly, in Non-Dep males, IL-6 increased sIPSC decay time to 110.0 ± 4.6% (one-sample t-test, $p = 0.042$) (Fig. 6B4). Taken together, these results suggest that in males, IL-6 decreases inhibitory drive during dependence and withdrawal by reducing presynaptic GABA release (reduced sIPSC frequencies) and has modest effects on postsynaptic $GABA_A$ receptor function (sIPSC amplitudes and kinetics) in all treatment groups tested, albeit at different levels of CIE-2BC exposure.

In contrast to males, exogenous IL-6 decreased the mean sIPSC frequency only in WD females (Fig. 6C & D). Specifically, IL-6 decreased sIPSC frequency to 65.0 ± 6.9% (one sample t-test, $p = 0.0001$) (Fig. 6D1). In females, IL-6 did not significantly alter the amplitude (Fig. 6D2) or rise time (Fig. 6D3) of any treatment

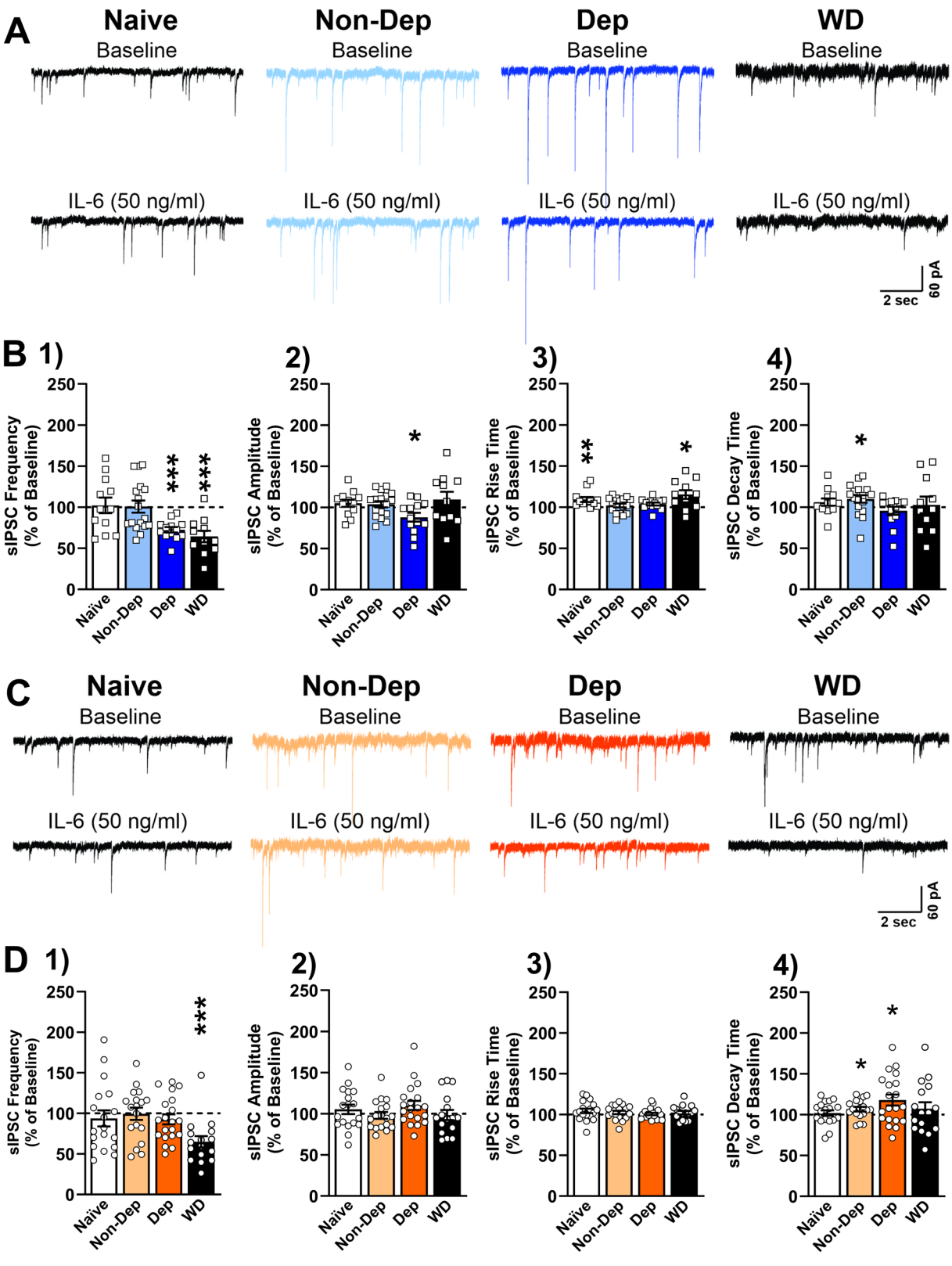

Fig. 6 (See legend on next page.)

(See figure on previous page.)

Fig. 6 IL-6 modulates CeA GABAergic transmission in a CIE-2BC treatment and sex-dependent manner. **A** Representative traces obtained from male CeA neurons before (baseline) and during bath application of IL-6 (50 ng/mL). **B** From left to right, the average IL-6 percent change from baseline of sIPSC frequency (1), amplitude (2), rise time (3) and decay time (4) of the CeA neurons recorded from alcohol naïve ($n = 12$ cells), Non-Dep ($n = 17$ cells), Dep (n = 13 cells) and WD ($n = 11$ cells) male mice. **C** Representative traces obtained from female CeA neurons before (baseline) and during bath application of IL-6 (50 ng/ml of IL-6). **D** From left to right, the average IL-6 percent change from baseline of sIPSC frequency (1), amplitude (2), rise time (3) and decay time (4) of the CeA neurons recorded from Naïve ($n = 18$ cells), Non-Dep ($n = 18$ cells), Dep ($n = 20$ cells) and WD ($n = 16$ cells) female mice. Results are expressed as mean ± SEM with points denoting individual cells and analyzed using two-tailed, one sample t tests (B1, B2, B4, D1-D4) or one sample Wilcoxon tests (B3). Significant differences are denoted by $^{*}p < 0.05$, $^{**}p < 0.01$ and $^{***}p < 0.001$. See Table S5 in Supplemental Materials for statistics relevant to each panel

group. Lastly, IL-6 increased the sIPSC decay time to 106.6 ± 2.8% (one sample t-test, $p = 0.026$) in Non-Dep females and to 118.0 ± 6.7% (one sample t-test, $p = 0.015$) in Dep females (Fig. 6D4). These results suggest that in females, IL-6 decreases inhibitory drive during withdrawal and has modest effects on postsynaptic $GABA_A$ receptor function (sIPSC decay) in Non-Dep and Dep treatment groups. Collectively, these data suggest that CIE-2BC induces neuroadaptive changes of the IL-6 system in a sex-dependent manner, with males exhibiting more pre- and postsynaptic effects compared to females.

Next, we recorded miniature IPSCs (mIPSCs, using 0.5 μM tetrodotoxin to block neuronal spiking through inhibition of sodium channels) to assess IL-6 effects on action-potential independent GABAergic transmission. We focused on the WD group where IL-6 had the most robust effect on reductions of GABA release in both sexes with comparison to the naïve group. We did not detect any significant differences in baseline mIPSC parameters across groups (Fig. S5). We found that IL-6 did not alter mIPSC frequency in naïve mice but significantly decreased mIPSC frequency in WD mice of both sexes (Fig. S6). Together, these data suggest that during withdrawal from alcohol, IL-6 signals through IL-6R and gp130 to activate downstream signaling pathways including JAK/STAT which results in a dampening of presynaptic GABAergic transmission, as evidenced by IL-6 induced decrease in sIPSCs and mIPSCs, which may lead to increased neuronal excitability [47] and contribute to circuit adaptations underlying negative reinforcement and alcohol dependence.

Blocking IL-6 signaling decreases excessive alcohol drinking in female mice

Given the substantial recruitment of IL-6 signaling components following chronic alcohol exposure, we next examined whether blocking IL-6 signaling would affect escalation of drinking, a motivational hallmark of alcohol dependence. Thus, we used a CIE-2BC model that reliably produces escalation of alcohol intake in Dep mice [48, 49, 51–54]. After dependence was induced (Fig. S7), we administered the anti-mouse IL-6 receptor antibody (IL-6R Ab) or isotype control (IgG2b) *i.p.*, 150 μg/200 μL per day for 7 days in Non-Dep and Dep male and female mice (Fig. 7A). In Non-Dep male mice, there was no significant effect of IL-6R Ab treatment, time, or their interaction on alcohol intake (Fig. 7B) or water intake (Fig. 7C). In Non-Dep female mice, there was a significant effect of time on alcohol intake (Fig. 7D; $F_{3.2,86.4} = 11.9$, $p < 0.0001$) but not water intake (Fig. 7E) and there were no effects of IL-6R Ab treatment or treatment x time interaction on either dependent measure (Fig. 7D&E). Like the Non-Dep males, in the Dep males there were no significant effects of IL-6R Ab treatment, time, or their interaction on alcohol (Fig. 7F) or water intake (Fig. 7G). However, there were significant effects of both IL-6R Ab treatment and time in Dep females (Fig. 7H; Treatment: $F_{1,23} = 5.1$, $p = 0.03$; Time: $F_{3.1,70.5} = 8.0$, $p = 0.0001$). Specifically, while overall alcohol intake escalated across the week, IL-6R Ab treatment reduced alcohol intake when compared to control (IgG2b treated) mice. There were no effects of IL-6R Ab treatment on water intake, time, or their interaction in Dep females (Fig. 7I) indicating that IL-6R Ab selectively reduced alcohol intake in Dep female mice.

Overall, our molecular, electrophysiological, and behavioral data support our primary hypothesis that alcohol dependence is associated with the functional activation of CeA IL-6 signaling in a sex-specific manner, and that blocking IL-6 signaling represents a promising strategy for reducing problematic alcohol use in the context of AUD.

Discussion

In this study, we observed a dysregulation of IL-6 signaling following alcohol consumption in the central amygdala in both clinical and preclinical settings. In total, our results determined that 1) IL-6 signaling pathways in human subjects with AUD are upregulated compared to controls, which further supports a role for neuroimmune activation in the pathogenesis of AUD [10–12, 14, 15], 2) genes in the IL-6 pathway are differentially regulated in the CeA of alcohol-exposed mice, 3) alcohol dependence significantly increases the number of IL-6-expressing CeA cells, particularly microglia, in both male and female mice, and IL-6-expressing neurons in dependent male mice, 4) IL-6 protein abundance is elevated in dependent females, accompanied by increases in other cytokines and immune-related signaling factors, 5) exogenous application of recombinant IL-6 decreases GABAergic synaptic transmission, with significant decreases in alcohol-dependent and withdrawn mice, and 6) blocking IL-6 signaling using an IL-6 receptor antibody significantly

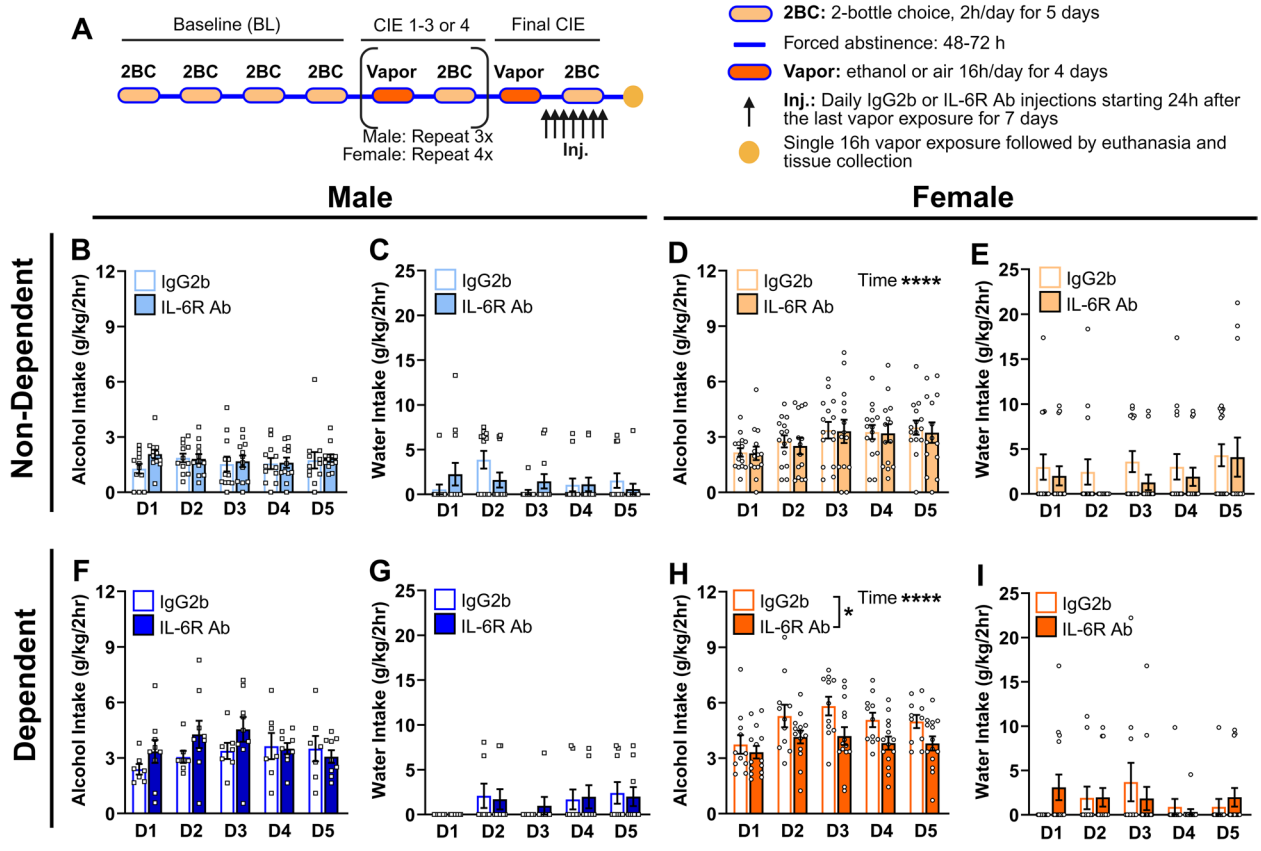

Fig. 7 Blocking IL-6 signaling decreases excessive alcohol drinking in female mice. Effects of IL-6R Ab on alcohol and water intake (g/kg/2 h) in Non-Dep and Dep male ($n = 40$) and female ($n = 56$) mice compared to the isotype control group (IgG2b) across the five treatment days (D1-5). **A** Experimental timeline for Cohort 3 mice injected with either IL-6R Ab or IgG2b control. For full experimental details, see methods section. **B** Alcohol intake in Non-Dep male mice. **C** Water intake in Non-Dep male mice. **D** Alcohol intake in Non-Dep female mice. **E** Water intake in Non-Dep female mice. **F** Alcohol intake in Dep male mice. **G** Water intake in Dep male mice. **H** Alcohol intake in Dep female mice. **I** Water intake in Dep female mice. Results are expressed as mean ± SEM and analyzed using two-way repeated measures ANOVA (**A-C**, **E–H** or mixed-effects model (**D**). Significant differences are denoted by $^{*}p < 0.05$ and $^{****}p < 0.0001$. See Table S5 in Supplemental Materials for statistics relevant to each panel

prevents the escalation of drinking in alcohol dependent female mice. Overall, these results suggest that alcohol modulates IL-6 signaling and targeting the IL-6 signaling pathway may represent a therapeutic strategy for alcohol use disorder in the future.

In human patients with AUD, chronic alcohol consumption results in a persistent increase in neuroimmune-related gene expression [94], while the intensity of neuroimmune response activation correlates with the amount of alcohol use over the lifetime [11, 21, 22]. Recently, we identified a variety of DEGs in the CeA of high vs. low drinking rhesus macaques, many of which were related to immune function and specifically, IL-6 function [95]. In accordance with these findings, we identified an upregulation of *IL6*, as well as multiple other immune-related genes including *IL1β*, chemokine ligands, and tumor necrosis factor receptor superfamily members in the CeA, indicating a strong inflammatory signature in the central amygdala of human subjects with AUD compared to controls without. These findings are consistent with studies showing enhanced glial activation and immune signaling in neurodegenerative conditions [96, 97]. Furthermore, a meta-analysis of 23 studies found significantly higher concentrations of *IL6* in people with AUD when compared to controls [98] as well as a separate systematic review and meta-analysis wherein *IL6* exhibited the strongest elevation among circulating cytokines in individuals with AUD [99]. Additionally, binge-drinkers exhibit increased serum *IL6* levels in comparison to social drinkers [31]. Other genes discovered, that are not directly immune-related, are associated with broader stress and inflammatory responses, emphasizing the critical role of *IL6* and associated pathways in AUD. Overall, our transcriptomic analyses of human CeA indicate that individuals with AUD exhibit a generalized neuroimmune activation that includes both neuronal and glial immune signaling consistent with similar findings across other neurodegenerative conditions [100–103].

Our clinical gene expression results were mirrored at the preclinical level following the CIE-2BC mouse model

of AUD. Specifically, there was predicted upregulation of *Il6* expression in CeA astrocytes of Dep mice as compared to Non-Dep mice, and increased *Il6* expression in microglia of Dep mice of both sexes as well as neurons in males. Data obtained using astrocyte-TRAP mice indicate that, while *Il6* mRNA levels were detected but filtered out of our analysis based on low read-counts in the astrocyte translating RNA fraction and, in the input, (bulk tissue) fraction, the IL-6 signaling pathway is upregulated in alcohol-dependent mice. This is demonstrated by increased *Il6ra* and *Il6st* expression in CeA astrocytes of Dep as compared to Non-Dep mice. Similarly, there was no difference in *Il6* expression in CeA astrocytes following dependence as assessed by RNAscope. Notably, *Il6ra* expression in CeA astrocytes of Dep females was significantly decreased in our RNAscope study. These results may indicate that although the number of CeA astrocytes producing *Il6ra* is decreased, the expression of *Il6ra* in the remaining *Il6ra*$^{+}$ astrocytes is increased. Further, these results identify neurons, astrocytes, and microglia as key players in the propagation of IL-6-initiated neuroinflammatory signaling. This is congruent with our findings on neuronal GABAergic transmission herein as well as our previous findings on CeA astrocyte-produced IL-6's role in stress-coping behaviors [47], and microglia-depletion induced prevention of alcohol escalation [104], respectively.

Alcohol consumption has been shown to increase IL-6 protein levels in mouse serum [105], in addition to hippocampal [105] (but see [106]), and spinal tissue [49] after chronic alcohol exposure, as well as in rat serum within a preclinical model of co-occurring AUD and post-traumatic stress exposure [79] and amygdala following acute ethanol challenge [107]. Here, we build on this prior work by examining how chronic alcohol exposure influences inflammatory cytokine abundance and function in the CeA. We found a broadly altered inflammatory signature in female mice. Specifically, we detected elevated levels of IL-6, IL-1β and IL-1α in Dep females when compared to both their naïve and Non-Dep counterparts as well as increased IFN-γ and TNF-α levels when compared to the Non-Dep group. In contrast, only Il-1β was significantly elevated in Dep males when compared to Non-Dep males. However, further examination of the signaling pathway in the CeA of alcohol-dependent male mice revealed an increase in IL-6 signaling, indicated by increases in STAT3 phosphorylation with no counter-regulatory changes in the level SOCS3 protein. SOCS3 is normally induced by IL-6/pSTAT activity in the brain to limit the function of this signaling axis. The current result suggests that CeA pSTAT signaling remains unchecked in the context of alcohol dependence, leading to a greater transcription of additional cytokines and potentially enduring pro-inflammatory state [24]. Notably, although SOCS3 protein levels were not upregulated in dependent male mice as compared to the non-dependent state, there was predicted upregulation of *Socs3* in dependent mouse astrocyte-specific TRAP-isolated translating mRNAs. Additionally, *SOCS3* was significantly upregulated in transcriptomic analysis of human postmortem tissue samples when compared to controls. This discrepancy may be due to translating efficiency (from genes to proteins), temporal dynamics of protein synthesis, or methodological differences such as assay sensitivity and cell types included (astrocyte vs. all cell types in the CeA). Taken together, these findings align with human research suggesting that female brains may be more susceptible to alcohol-induced damage than male brains [108]. Further, at the preclinical level, it's been reported that alcohol triggers stronger neuroinflammatory effects in female mice [109]. We speculate that this more sever neuroimmune activation in females may be driven, at least in part by the higher alcohol intake in females as compared to males.

Pro- and anti-inflammatory cytokines play a critical role in regulating immune responses but are also important for neuronal physiological function in both normal and pathological conditions [15, 16]. We have demonstrated profound changes at CeA GABAergic synapses in response to anti-inflammatory IL-10 [37], pro-inflammatory IL-1β [48, 110–113], and IL-18 [74] exposure, supporting a role of cytokines in influencing neuronal function and synaptic transmission in rodents and rhesus macaques. In the temporal cortex, exogenous IL-6 reduced the amplitude of evoked IPSCs [114]. In contrast, IL-6 increased GABA-mediated sIPSC amplitudes in the basolateral amygdala of naïve adult rats, but not in adolescent rats [115]. Recently, we found that IL-6 decreased CeA GABA release in both control and alcohol drinking rhesus macaques of both sexes, whereas the IL-6 induced postsynaptic $GABA_A$ receptor mediated effects were sex- and alcohol-specific [95]. Here we report that in mice, IL-6 significantly reduced presynaptic spontaneous GABA release (sIPSC frequency) in CeA neurons of Dep males and WD males and females. The IL-6-induced effects on postsynaptic $GABA_A$ receptor mediated properties were variable across sex and condition. Specifically, IL-6 significantly reduced amplitude (naïve males only), increased rise time (naïve and WD males), and increased decay time (Non-Dep males and females & Dep females) of postsynaptic inhibitory currents. IL-6 also significantly decreased presynaptic action potential-independent GABA release (mIPSC frequency) in CeA neurons of WD males and females. Detectable levels of IL-6R and gp130 have been found at both the pre- and post-synapse of neurons [93]. In addition, the IL-6R is found on astrocytes and microglia. Therefore, IL-6 could be working directly through neuronal IL-6Rs to alter synaptic

release of GABA (as evidenced by the reduction in sIPSCs) and/or $GABA_A$ receptor function (as evidenced by the changes in rise and decay time). However, IL-6 could also be working indirectly through astrocytic/microglial IL6-Rs to alter non-synaptic release of other cytokines and/or neuromodulators to effect GABAergic signaling (as evidenced by the reduction in mIPSCs). Although speculative, we suggest that the observed changes in inhibitory signaling likely result from a combination of the above mechanisms. Overall, these data suggest that IL-6 modulation of the GABAergic transmission in the CeA is mediated via pre-synaptic mechanisms in a similar manner (reduction of both network dependent and vesicular GABA release), whereas the IL-6 postsynaptic actions are more related to sex- and alcohol in a treatment-specific manner, similar to what was observed in rhesus macaques [95].

IL-6R Antibodies have received U.S. Food and Drug Administration (FDA) approval for autoimmune and inflammatory conditions. Specifically, Toclizumab and Sarilumab are approved for rheumatoid arthritis, while Toclizumab is also approved for juvenile idiopathic arthritis, giant cell arteritis, and cytokine release syndrome [116, 117]. IL-6R Antibodies have additionally been studied for optical, coronary, and kidney diseases among other disorders [118, 119]. We extend these studies to also examine the role of IL-6 signaling in AUD and related comorbidities. Previously, we found that IL-6 is involved in stress-coping behaviors using transgenic mice with elevated levels of IL-6 [47] and a trend for IL-6R Ab alleviation of chronic alcohol-induced mechanical allodynia in Dep male mice [49]. Here, we identified a critical, sex-dependent role for IL-6 in modifying dependence-induced escalation of alcohol drinking. Specifically, we found that peripheral administration of an IL-6R Ab was sufficient to prevent escalated alcohol drinking in Dep female mice without altering Non-Dep mice nor overall alcohol or water consumption. These data suggest that IL-6 specifically impacts the motivation to consume alcohol in the context of dependence. This has important implications when considering sex differences in both motivational and biological mechanisms, including alcohol-induced changes in neurotransmission and neuroimmune signaling [15, 55, 56, 107, 120–128]. Interestingly, this sex-specific result could be explained by the observed increase in central amygdalar IL-6 in Dep female mice, which was absent in Dep males and may be due at least in part to greater alcohol consumption in females as compared to males. Taken together, these findings have promising therapeutic implications for the use of IL-6R Abs. However, they underline the need for future study to empirically determine whether the observed efficacy of IL-6R Ab in females only is due to inherent sex differences or instead dependent on the increased alcohol intake displayed by female mice. Additional studies modifying the course of administration (e.g., timing and dose) could yield a more robust effect, particularly in male mice. Notably, *i.p.* administration of IL-6R Ab has been used in preclinical models of CNS-related disorders [29, 49, 81–88]. Further, in the CSF from mice undergoing the same CIE-2BC model and IL-6R Ab injection timeline used herein, we detected a rat IgG2b peptide sequence in both Non-Dep and Dep mice indicating that the rat anti-mouse IL-6R Ab used in this study passed the blood–brain barrier [129]. Additionally, while not tested in this study, it would be critical to determine whether the IL-6R Ab could reduce negative affective states such as anxiety- and depressive-like symptoms, which are hypothesized to underlie negative reinforcement for continued alcohol use in individuals with AUD [9]. Altogether, these findings highlight the potential of IL-6 receptor blockade as a novel therapeutic approach for AUD and potential comorbid conditions.

We acknowledge several limitations that could enhance this conceptual framework, though addressing them lies beyond the scope of this report. First, our study included the use of Aldh1l1-eGFP/Rpl10a mice, which allow for the pull-down of astrocyte-specific RNA using the TRAP procedure based on evidence that astrocyte-specific production of IL-6 contributes to increased alcohol withdrawal susceptibility and decreased stress-coping behaviors [46, 47]. Similar mice have been developed to assess microglia-specific contributions as well [130, 131]. Based on our microglia depletion studies [13], microglial IL-6 signaling may be predominant in the escalation of drinking in male mice. Accordingly, examination of microglia-specific contributions will be reported in due course. Second, we evaluated the effects of a single dose of IL-6R Ab administered through repeated *i.p.* injections on the escalation of alcohol drinking based on previous work [29, 49]. However, a larger dose of IL-6R Ab may be needed to yield a significant effect on chronic-alcohol induced escalation of drinking in male mice. Although not feasible within the constraints of the current experimental timeline, generating a full dose–response curve is warranted. Third, earlier reports indicate that IL-6 levels fluctuate across the estrous cycle [132, 133]. Further investigation is required to clarify how IL-6 changes across the estrous cycle in our CIE-2BC mouse model and how these variations may affect sensitivity to IL-6R Ab treatment. Fourth, differential expression analysis of the postmortem human CeA samples was performed on pooled male and female samples because the study lacked sufficient power for sex-stratified analyses. Fifth, our inability to directly determine the relative contributions of neuronal versus glial IL-6 signaling pathways to the observed changes in GABAergic synaptic transmission is a limitation of the present study. While we anticipate

that the observed alterations in inhibitory signaling likely result from a combination of mechanisms, future studies will be needed to delineate this. Finally, to make our experimental design manageable, we did not include all four treatment groups or both sexes in every experiment. Accordingly, we emphasized comparisons against the alcohol-dependent group as prioritized by ingenuity pathway analysis.

Abbreviations

AUD	Alcohol use disorder
IL-6	Interleukin-6
gp130	Membrane glycoprotein 130
IL6ST	IL-6 cytokine family signal transducer
sIL-6R	Soluble IL-6 receptor
JAK/STAT	Janus Kinase/Signal Transducer and Activator of Transcription
MAPK	Mitogen-Activated Protein Kinase
PI3K/AKT	Phosphoinositide 3-Kinase/Protein Kinase B
IL-6R Ab	IL-6 receptor antibody
IL-6R	IL-6 receptor subunit
Il6ra	Gene encoding IL-6 receptor subunit (IL-6R)
Il6st	Gene encoding membrane glycoprotein130/IL-6 cytokine family signal transducer (gp130/IL6ST)
Stat3	Gene encoding signal transducer and activator of transcription 3 (STAT3)
Socs3	Gene encoding suppressor of cytokine signaling 3 (SOCS3)
CeA	Central amygdala
SOCS3	Suppressor of cytokine signaling 3
CIE-2BC	Chronic-intermittent ethanol two-bottle choice paradigm
TRAP	Translating ribosome affinity purification
BL	Baseline
Non-Dep	Non-dependent
Dep	Dependent
WD	Withdrawal
EtOH	Ethanol
i.p.	Intraperitoneally
BAL	Blood alcohol level
IP	Immunoprecipitated
FC	Fold change
IPA	Ingenuity pathway analysis
PBS	Phosphate buffered saline
Itgam	Gene encoding integrin alpha M
Gfap	Gene encoding glial fibrillary acidic protein
Rbfox3	Gene encoding RNA-binding protein FOX-1 homolog 3
IL-1β	Interleukin-1β
IL-1α	Interleukin-1α
IFN-γ	Interferon-γ
TNF-α	Tumor necrosis factor-α
IL-10	Interleukin-10
IL-17	Interleukin-17
MCP-1	Monocyte chemoattractant protein-1
sIPSCs	Spontaneous inhibitory postsynaptic currents
mIPSCs	Miniature inhibitory postsynaptic currents
aCSF	Artificial cerebrospinal fluid
CNS	Central nervous system
DEGs	Differentially expressed genes
LIF	Leukemia inhibitory factor
CCL2	C-C motif chemokine ligand 2
PF4	Platelet factor 4
TNFRSF12A	Tumor necrosis factor receptor superfamily member 12A
FOSL1	FOS-like antigen 1
RAET1L	Retinoic acid early transcript 1L
HLA-A	Major histocompatibility complex, class 1, A
CD1D	Antigen-presenting glycoprotein CD1d
SFN	14-3–3 Protein sigma
Socs1	Gene encoding suppressor of cytokine signaling 1
Tnfrsd1a	Gene encoding tumor necrosis and factor receptor superfamily member 1a
Pik3c	Gene encoding phosphatidylinositol-4-phosphate 3-kinase catalytic subunit
Pik3r	Gene encoding phosphoinositide-3-kinase regulatory subunit
pSTAT3	Phosphorylated STAT3

Supplementary Information

The online version contains supplementary material available at https://doi.org/10.1186/s12974-026-03868-2.

Supplementary Material 1.

Acknowledgements

We thank Dr. Valentina Vozella, Dr. Paula Bianchi, and Dr. Alexia Anjos-Santos for their supporting technical contributions.

Authors' contributions

All authors contributed to the intellectual discussion of the study conception and design, and data interpretation. Material preparation, electrophysiological data collection and analyses were performed by CE, BC, LR, SK, RV, CSO, MB, and MR; Human RNAseq data collection and analysis were performed by NAS and RDM; Luminex assay were performed and analyzed by CMS and BC, Western blot assays were performed and analyzed by JAC-R, TF-S and SE; TRAP studies were performed and analyzed by JGH and MG; RNAscope/ISH were performed and analyzed by VB, SK and MP; Material preparation, behavioral studies and management of cohorts were performed by TN, AJR, and MB; CMS, MB, and MR wrote the manuscript. All authors commented on previous versions of the manuscript. All authors read and approved of the final manuscript.

Funding

Research reported in this publication was supported by the National Institute on Alcohol Abuse and Alcoholism (NIAAA) of the National Institutes of Health under award numbers: AA013498 (MR), AA017447 (MR), AA027700 (MR), P60 AA006420 (MR), AA029841 (MR), AA012404 (RDM), U01AA020926 (RDM), R01AA025996 (SE), K99AA031718 (BC), T32AA007456 (CS, CE, LR, and BC), U01AA029965 (MG), P60AA010760 (MG), and R01AA029486 (MG) as well as the National Institute on Drug Abuse (NIDA) of the National Institutes of Health under award number: R21DA060442 (MG). NIAAA and NIDA had no role in study design, data collection, data analysis, manuscript preparation, or the decision to submit the manuscript for publication. Additional support was provided by the Schimmel Family Chair, VA Merit Review Award I01BX001819 (MG), and by facilities and resources at the Portland VA Health Care System (MG). The contents of this article do not represent the views of the United States Department of Veterans Affairs or the United States government.

Data availability

RNA-seq data resulting from postmortem human central amygdala samples are available under BioProject #PRJNA551908. RNA-seq data resulting from mouse Astrocyte-TRAP CIE-2BC samples are available at the National Center for Biotechnology Information Gene Expression Omnibus site (https://www.ncbi.nlm.nih.gov/geo/) under accession GSE325031. All other data are available upon reasonable request made to the corresponding author.

Declarations

Competing interests

The authors declare no competing interests.

Received: 3 March 2026 / Accepted: 7 May 2026
Published online: 22 May 2026

References

1. Koob GF, Buck CL, Cohen A, Edwards S, Park PE, Schlosburg JE, et al. Addiction as a stress surfeit disorder. Neuropharmacology. 2014;76(Pt B(0 0)):370–82.
2. Koob GF, Le Moal M. Addiction and the brain antireward system. Annu Rev Psychol. 2008;59:29–53.

3. Grant BF, Goldstein RB, Saha TD, Chou SP, Jung J, Zhang H, et al. Epidemiology of DSM-5 alcohol use disorder: results from the national epidemiologic survey on alcohol and related conditions III. JAMA Psychiat. 2015;72(8):757–66.
4. Grant BF, Chou SP, Saha TD, Pickering RP, Kerridge BT, Ruan WJ, et al. Prevalence of 12-month alcohol use, high-risk drinking, and DSM-IV alcohol use disorder in the United States, 2001–2002 to 2012–2013: results from the national epidemiologic survey on alcohol and related conditions. JAMA Psychiat. 2017;74(9):911–23.
5. Grant BF, Stinson FS, Dawson DA, Chou SP, Dufour MC, Compton W, et al. Prevalence and co-occurrence of substance use disorders and independent mood and anxiety disorders: results from the National epidemiologic survey on alcohol and related conditions. Arch Gen Psychiatry. 2004;61(8):807–16.
6. Guinle MIB, Sinha R. The role of stress, trauma, and negative affect in alcohol misuse and alcohol use disorder in women. Alcohol Res. 2020;40(2):05.
7. Sun N, Cassell MD. Intrinsic GABAergic neurons in the rat central extended amygdala. J Comp Neurol. 1993;330(3):381–404.
8. Veinante P, Freund-Mercier MJ. Intrinsic and extrinsic connections of the rat central extended amygdala: an in vivo electrophysiological study of the central amygdaloid nucleus. Brain Res. 1998;794(2):188–98.
9. Koob GF. The dark side of emotion: the addiction perspective. Eur J Pharmacol. 2015;753:73–87.
10. Mayfield J, Ferguson L, Harris RA. Neuroimmune signaling: a key component of alcohol abuse. Curr Opin Neurobiol. 2013;23(4):513–20.
11. Robinson G, Most D, Ferguson LB, Mayfield J, Harris RA, Blednov YA. Neuroimmune pathways in alcohol consumption: evidence from behavioral and genetic studies in rodents and humans. Int Rev Neurobiol. 2014;118:13–39.
12. Montesinos J, Alfonso-Loeches S, Guerri C. Impact of the innate immune response in the actions of ethanol on the central nervous system. Alcohol Clin Exp Res. 2016;40(11):2260–70.
13. Warden AS, Wolfe SA, Khom S, Varodayan FP, Patel RR, Steinman MQ, et al. Microglia control escalation of drinking in alcohol dependent mice: genomic and synaptic drivers. Biol Psychiatry. 2020. https://doi.org/10.1016/j.biopsych.2020.05.011.
14. Crews FT, Walter TJ, Coleman LG Jr., Vetreno RP. Toll-like receptor signaling and stages of addiction. Psychopharmacology. 2017;234(9–10):1483–98.
15. Cruz B, Borgonetti V, Bajo M, Roberto M. Sex-dependent factors of alcohol and neuroimmune mechanisms. Neurobiol Stress. 2023;26:100562.
16. Roberto M, Patel RR, Bajo M. Ethanol and cytokines in the central nervous system. Handb Exp Pharmacol. 2018;248:397–431.
17. Guizzetti M, Mangieri RA, Ezerskiy LA, Hashimoto JG, Bajo M, Farris SP, et al. Astrocytes and alcohol throughout the lifespan. Biol Psychiatry. 2026;99(1):9–20.
18. Nentwig TB, Obray JD, Kruyer A, Wilkes ET, Vaughan DT, Scofield MD, et al. Central amygdala astrocyte plasticity underlies GABAergic dysregulation in ethanol dependence. Transl PsychiatrybioRxiv. 2025;15(1):132.
19. Coleman LG Jr, Crews F. Innate immune signaling and alcohol use disorders. 2018;248:369–96.
20. Crews FT, Lawrimore CJ, Walter TJ, Coleman LG Jr. The role of neuroimmune signaling in alcoholism. Neuropharmacology. 2017;122:56–73.
21. Crews FT, Vetreno RP. Neuroimmune basis of alcoholic brain damage. Int Rev Neurobiol. 2014;118:315–57.
22. Crews FT, Vetreno RP. Mechanisms of neuroimmune gene induction in alcoholism. Psychopharmacology. 2016;233(9):1543–57.
23. Schett G. Physiological effects of modulating the interleukin-6 axis. Rheumatology (Oxford). 2018;57(suppl_2):ii43–50.
24. Hodes GE, Menard C, Russo SJ. Integrating interleukin-6 into depression diagnosis and treatment. Neurobiol Stress. 2016;4:15–22.
25. Mullberg J, Schooltink H, Stoyan T, Gunther M, Graeve L, Buse G, et al. The soluble interleukin-6 receptor is generated by shedding. Eur J Immunol. 1993;23(2):473–80.
26. Levin SG, Godukhin OV. Modulating effect of cytokines on mechanisms of synaptic plasticity in the brain. Biochemistry (Mosc). 2017;82(3):264–74.
27. Rothaug M, Becker-Pauly C, Rose-John S. The role of interleukin-6 signaling in nervous tissue. Biochim Biophys Acta. 2016;1863(6 Pt A):1218–27.
28. Tanaka T, Kishimoto T. The biology and medical implications of interleukin-6. Cancer Immunol Res. 2014;2(4):288–94.
29. Murakami T, Kanchiku T, Suzuki H, Imajo Y, Yoshida Y, Nomura H, et al. Anti-interleukin-6 receptor antibody reduces neuropathic pain following spinal cord injury in mice. Exp Ther Med. 2013;6(5):1194–8.
30. Sery O, Hladilova R, Novotny M, Hribkova H, Znojil V, Zvolsky P. Association between -174 G/C polymorphism of interleukin-6 gene and alcoholism. Acta Neuropsychiatr. 2003;15(5):257–61.
31. Blaine SK, Ridner CM, Campbell BR, Crone L, Claus ED, Wilson JR, et al. IL-6, but not TNF-alpha, response to alcohol cues and acute consumption associated with neural cue reactivity, craving, and future drinking in binge drinkers. Brain Behav Immun Health. 2023;31:100645.
32. Blaine SK, Seo D, Sinha R. Peripheral and prefrontal stress system markers and risk of relapse in alcoholism. Addict Biol. 2015. https://doi.org/10.1111/adb.12320.
33. Blaine SK, Sinha R. Alcohol, stress, and glucocorticoids: from risk to dependence and relapse in alcohol use disorders. Neuropharmacology. 2017;122:136–47.
34. Egli M. Advancing pharmacotherapy development from preclinical animal studies. Handb Exp Pharmacol. 2018;248:537–78.
35. Osterndorff-Kahanek E, Ponomarev I, Blednov YA, Harris RA. Gene expression in brain and liver produced by three different regimens of alcohol consumption in mice: comparison with immune activation. PLoS ONE. 2013;8(3):e59870.
36. Ponomarev I, Wang S, Zhang L, Harris RA, Mayfield RD. Gene coexpression networks in human brain identify epigenetic modifications in alcohol dependence. J Neurosci. 2012;32(5):1884–97.
37. Patel RR, Wolfe SA, Bajo M, Abeynaike S, Pahng A, Borgonetti V, et al. IL-10 normalizes aberrant amygdala GABA transmission and reverses anxiety-like behavior and dependence-induced escalation of alcohol intake. Prog Neurobiol. 2021;199:101952.
38. Xu J, Ma HY, Liu X, Rosenthal S, Baglieri J, McCubbin R, et al. Blockade of IL-17 signaling reverses alcohol-induced liver injury and excessive alcohol drinking in mice. JCI Insight. 2020. https://doi.org/10.1172/jci.insight.131277.
39. Erickson EK, DaCosta AJ, Mason SC, Blednov YA, Mayfield RD, Harris RA. Cortical astrocytes regulate ethanol consumption and intoxication in mice. Neuropsychopharmacology. 2021;46(3):500–8.
40. Erickson EK, Blednov YA, Harris RA, Mayfield RD. Glial gene networks associated with alcohol dependence. Sci Rep. 2019;9(1):10949.
41. Erickson EK, Grantham EK, Warden AS, Harris RA. Neuroimmune signaling in alcohol use disorder. Pharmacol Biochem Behav. 2019;177:34–60.
42. Kimpel MW, Strother WN, McClintick JN, Carr LG, Liang T, Edenberg HJ, et al. Functional gene expression differences between inbred alcohol-preferring and -non-preferring rats in five brain regions. Alcohol. 2007;41(2):95–132.
43. Mulligan MK, Ponomarev I, Hitzemann RJ, Belknap JK, Tabakoff B, Harris RA, et al. Toward understanding the genetics of alcohol drinking through transcriptome meta-analysis. Proc Natl Acad Sci U S A. 2006;103(16):6368–73.
44. Blednov YA, Ponomarev I, Geil C, Bergeson S, Koob GF, Harris RA. Neuroimmune regulation of alcohol consumption: behavioral validation of genes obtained from genomic studies. Addict Biol. 2012;17(1):108–20.
45. Chourbaji S, Urani A, Inta I, Sanchis-Segura C, Brandwein C, Zink M, et al. IL-6 knockout mice exhibit resistance to stress-induced development of depression-like behaviors. Neurobiol Dis. 2006;23(3):587–94.
46. Hernandez RV, Puro AC, Manos JC, Huitron-Resendiz S, Reyes KC, Liu K, et al. Transgenic mice with increased astrocyte expression of IL-6 show altered effects of acute ethanol on synaptic function. Neuropharmacology. 2016;103:27–43.
47. Roberts AJ, Khom S, Bajo M, Vlkolinsky R, Polis I, Cates-Gatto C, et al. Increased IL-6 expression in astrocytes is associated with emotionality, alterations in central amygdala GABAergic transmission, and excitability during alcohol withdrawal. Brain Behav Immun. 2019;82:188–202.
48. Patel RR, Khom S, Steinman MQ, Varodayan FP, Kiosses WB, Hedges DM, et al. IL-1beta expression is increased and regulates GABA transmission following chronic ethanol in mouse central amygdala. Brain Behav Immun. 2019;75:208–19.
49. Borgonetti V, St Onge CM, Cruz B, Zalfa C, Nadav T, Roberts AJ, et al. Targeting IL-6 as a novel therapeutic approach for alcohol abstinence - related mechanical allodynia. Neuropharmacology. 2025;278:110584.
50. Varodayan FP, Pahng AR, Davis TD, Gandhi P, Bajo M, Steinman MQ, et al. Chronic ethanol induces a pro-inflammatory switch in interleukin-1beta regulation of GABAergic signaling in the medial prefrontal cortex of male mice. Brain Behav Immun. 2023;110:125–39.
51. Gorini G, Roberts AJ, Mayfield RD. Neurobiological signatures of alcohol dependence revealed by protein profiling. PLoS ONE. 2013;8(12):e82656.
52. Griffin Iii WC. Alcohol dependence and free-choice drinking in mice. Alcohol. 2014;48(3):287–93.
53. Hashimoto JG, Mangieri RA, Roberts AJ, Lime T, Davis BA, Carbone L, et al. Alcohol dependence-induced astrocyte immune activation in the nucleus accumbens. Neurobiol Dis. 2025;217:107171.

54. Becker HC, Lopez MF. Increased ethanol drinking after repeated chronic ethanol exposure and withdrawal experience in C57BL/6 mice. Alcohol Clin Exp Res. 2004;28(12):1829–38.
55. Peltier MR, Verplaetse TL, Mineur YS, Petrakis IL, Cosgrove KP, Picciotto MR, et al. Sex differences in stress-related alcohol use. Neurobiol Stress. 2019;10:100149.
56. Pollard MS, Tucker JS, Green HD Jr. changes in adult alcohol use and consequences during the COVID-19 pandemic in the US. JAMA Netw Open. 2020;3(9):e2022942.
57. Doyle JP, Dougherty JD, Heiman M, Schmidt EF, Stevens TR, Ma G, et al. Application of a translational profiling approach for the comparative analysis of CNS cell types. Cell. 2008;135(4):749–62.
58. Heiman M, Schaefer A, Gong S, Peterson JD, Day M, Ramsey KE, et al. A translational profiling approach for the molecular characterization of CNS cell types. Cell. 2008;135(4):738–48.
59. Rao X, Thapa KS, Chen AB, Lin H, Gao H, Reiter JL, et al. Allele-specific expression and high-throughput reporter assay reveal functional genetic variants associated with alcohol use disorders. Mol Psychiatry. 2021;26(4):1142–51.
60. Kapoor M, Wang JC, Farris SP, Liu Y, McClintick J, Gupta I, et al. Analysis of whole genome-transcriptomic organization in brain to identify genes associated with alcoholism. Transl Psychiatry. 2019;9(1):89.
61. Hashimoto JG, Gonzalez AE, Gorham N, Barbour Z, Roberts AJ, Day LZ, et al. Astrocyte reactivity by alcohol dependence in the central amygdala. bioRxiv. 2026:2026.04.02.716159.
62. Frankin KB, Paxinos G. The mouse brain in stereotaxic coordinates (3rd ed.). Academic Press. 2008.
63. Hashimoto JG, Margolies N, Zhang X, Karpf J, Song Y, Gorham N, et al. Astrocyte extracellular matrix modulates neuronal dendritic development. Glia. 2025;73(8):1589–607.
64. Dobin A, Davis CA, Schlesinger F, Drenkow J, Zaleski C, Jha S, et al. STAR: ultrafast universal RNA-seq aligner. Bioinformatics. 2013;29(1):15–21.
65. Love MI, Huber W, Anders S. Moderated estimation of fold change and dispersion for RNA-seq data with DESeq2. Genome Biol. 2014;15(12):550.
66. Kawa AB, Hashimoto JG, Beutler MM, Guizzetti M, Wolf ME. Changes in nucleus accumbens core translatome accompanying incubation of cocaine craving. Neuropsychopharmacology. 2025;50(8):1305–16.
67. Wang X, Spandidos A, Wang H, Seed B. PrimerBank: a PCR primer database for quantitative gene expression analysis, 2012 update. Nucleic Acids Res. 2012;40(Database issue):D1144–9.
68. Khom S, Borgonetti V, Vozella V, Kirson D, Rodriguez L, Gandhi P, et al. Glucocorticoid receptors regulate central amygdala GABAergic synapses in Marchigian-Sardinian alcohol-preferring rats. Neurobiol Stress. 2023;25:100547.
69. Khom S, Wolfe SA, Patel RR, Kirson D, Hedges DM, Varodayan FP, et al. Alcohol Dependence and Withdrawal Impair Serotonergic Regulation of GABA Transmission in the Rat Central Nucleus of the Amygdala. J Neurosci. 2020;40(36):6842–53.
70. Wolfe SA, Contet C, Roberto M. Characterization of corticotropin-releasing factor receptor 1 expressing neurons in the central nucleus of the amygdala. Alcohol Clin Exp Res. 2018;42(S1):212A.
71. Anjos-Santos A, Erikson CM, Flores-Ramirez FJ, Rodriguez L, Barchiesi R, Vozella V, et al. Noradrenaline Modulates Central Amygdala GABA transmission and alcohol drinking in female rats. Biol Psychiatry. 2026;99(1):21–33.
72. Varodayan FP, Patel RR, Matzeu A, Wolfe SA, Curley DE, Khom S, et al. The amygdala noradrenergic system is compromised with alcohol use disorder. Biol Psychiatry. 2022;91(12):1008–18.
73. Agoglia AE, Zhu M, Ying R, Sidhu H, Natividad LA, Wolfe SA, et al. Corticotropin-releasing factor receptor-1 neurons in the lateral amygdala display selective sensitivity to acute and chronic ethanol exposure. eNeuro. 2020. https://doi.org/10.1523/ENEURO.0420-19.2020.
74. Borgonetti V, Cruz B, Vozella V, Khom S, Steinman MQ, Bullard R, et al. IL-18 signaling in the rat central amygdala is disrupted in a comorbid model of post-traumatic stress and alcohol use disorders. Cells. 2023. https://doi.org/10.3390/cells12151943. In Press.
75. Wolfe SA, Sidhu H, Patel RR, Kreifeldt M, D'Ambrosio SR, Contet C, et al. Molecular, morphological, and functional characterization of corticotropin-releasing factor receptor 1-expressing neurons in the central nucleus of the amygdala. eNeuro. 2019;6(3):ENEURO.0087–19.2019 .
76. Jones TR, Kang IH, Wheeler DB, Lindquist RA, Papallo A, Sabatini DM, et al. Cell profiler analyst: data exploration and analysis software for complex image-based screens. BMC Bioinformatics. 2008;9:482.
77. Cruz B, Vozella V, Borgonetti V, Bullard R, Bianchi PC, Kirson D, et al. Chemogenetic inhibition of central amygdala CRF-expressing neurons decreases alcohol intake but not trauma-related behaviors in a rat model of post-traumatic stress and alcohol use disorder. Mol Psychiatry. 2024. https://doi.org/10.1038/s41380-024-02514-8.
78. Cruz B, Vozella V, Carper BA, Xu JC, Kirson D, Hirsch S, et al. FKBP5 inhibitors modulate alcohol drinking and trauma-related behaviors in a model of comorbid post-traumatic stress and alcohol use disorder. Neuropsychopharmacology. 2023;48(8):1144–54.
79. Steinman MQ, Kirson D, Wolfe SA, Khom S, D'Ambrosio SR, Spierling Bagsic SR, et al. Importance of sex and trauma context on circulating cytokines and amygdalar GABAergic signaling in a comorbid model of posttraumatic stress and alcohol use disorders. Mol Psychiatry. 2021;26(7):3093–107.
80. Siddiqi MT, Podder D, Pahng AR, Athanason AC, Nadav T, Cates-Gatto C, et al. Prefrontal cortex glutamatergic adaptations in a mouse model of alcohol use disorder. Addict Neurosci. 2023;9:100137.
81. Backstrom F, Ahl M, Wickham J, Ekdahl CT. Reduced epilepsy development in synapsin 2 knockout mice with autistic behavior following early systemic treatment with interleukin-6 receptor antibody. Epilepsy Res. 2023;191:107114.
82. Mukaino M, Nakamura M, Yamada O, Okada S, Morikawa S, Renault-Mihara F, et al. Anti-IL-6-receptor antibody promotes repair of spinal cord injury by inducing microglia-dominant inflammation. Exp Neurol. 2010;224(2):403–14.
83. Okada S, Nakamura M, Mikami Y, Shimazaki T, Mihara M, Ohsugi Y, et al. Blockade of interleukin-6 receptor suppresses reactive astrogliosis and ameliorates functional recovery in experimental spinal cord injury. J Neurosci Res. 2004;76(2):265–76.
84. Guptarak J, Wanchoo S, Durham-Lee J, Wu Y, Zivadinovic D, Paulucci-Holthauzen A, et al. Inhibition of IL-6 signaling: a novel therapeutic approach to treating spinal cord injury pain. Pain. 2013;154(7):1115–28.
85. Guerrero AR, Uchida K, Nakajima H, Watanabe S, Nakamura M, Johnson WE, et al. Blockade of interleukin-6 signaling inhibits the classic pathway and promotes an alternative pathway of macrophage activation after spinal cord injury in mice. J Neuroinflammation. 2012;9:40.
86. Kobayashi M, Tamari K, Miyamura T, Takeuchi K. Blockade of interleukin-6 receptor suppresses inflammatory reaction and facilitates functional recovery following olfactory system injury. Neurosci Res. 2013;76(3):125–32.
87. Wei J, Sun C, Liu C, Zhang Q. Effects of rat anti-mouse interleukin-6 receptor antibody on the recovery of cognitive function in stroke mice. Cell Mol Neurobiol. 2018;38(2):507–15.
88. Zhang JC, Yao W, Dong C, Yang C, Ren Q, Ma M, et al. Blockade of interleukin-6 receptor in the periphery promotes rapid and sustained antidepressant actions: a possible role of gut-microbiota-brain axis. Transl Psychiatry. 2017;7(5):e1138.
89. Mora P, Laisne M, Bourguignon C, Rouault P, Jaspard-Vinassa B, Maitre M, et al. Astrocytic DLL4-NOTCH1 signaling pathway promotes neuroinflammation via the IL-6-STAT3 axis. J Neuroinflammation. 2024;21(1):258.
90. Patani R, Hardingham GE, Liddelow SA. Functional roles of reactive astrocytes in neuroinflammation and neurodegeneration. Nat Rev Neurol. 2023;19(7):395–409.
91. Varodayan FP, Sidhu H, Kreifeldt M, Roberto M, Contet C. Morphological and functional evidence of increased excitatory signaling in the prelimbic cortex during ethanol withdrawal. Neuropharmacology. 2018;133:470–80.
92. Sidhu H, Kreifeldt M, Contet C. Affective disturbances during withdrawal from chronic intermittent ethanol inhalation in C57BL/6J and DBA/2J male mice. Alcohol Clin Exp Res. 2018;42(7):1281–90.
93. D'Arcangelo G, Tancredi V, Onofri F, D'Antuono M, Giovedi S, Benfenati F. Interleukin-6 inhibits neurotransmitter release and the spread of excitation in the rat cerebral cortex. Eur J Neurosci. 2000;12(4):1241–52.
94. Crews FT, Sarkar DK, Qin L, Zou J, Boyadjieva N, Vetreno RP. Neuroimmune function and the consequences of alcohol exposure. Alcohol Res. 2015;37(2):331–41, 44–51.
95. Bajo M, Gandhi P, Fei SS, Yu Y, Gao L, Khadka R, et al. Chronic alcohol consumption sex-dependently affects IL-6 modulation of GABAergic synapses in the central amygdala of rhesus macaques. Brain Behav Immun. 2025;132:106227.
96. Friske MM, Torrico EC, Haas MJW, Borruto AM, Giannone F, Hade AC, et al. A systematic review and meta-analysis on the transcriptomic signatures in alcohol use disorder. Mol Psychiatry. 2025;30(1):310–26.
97. Warden AS, Salem NA, Brenner E, Sutherland GT, Stevens J, Kapoor M, et al. Integrative Genomics Approach Identifies Glial Transcriptomic Dysregulation and Risk in the Cortex of Individuals With Alcohol Use Disorder. Biol Psychiatry. 2026;99(1):34–48.

98. Moura HF, Hansen F, Galland F, Silvelo D, Rebelatto FP, Ornell F, et al. Inflammatory cytokines and alcohol use disorder: systematic review and meta-analysis. Braz J Psychiatry. 2022;44(5):548–56.
99. Adams C, Conigrave JH, Lewohl J, Haber P, Morley KC. Alcohol use disorder and circulating cytokines: a systematic review and meta-analysis. Brain Behav Immun. 2020;89:501–12.
100. Gao C, Jiang J, Tan Y, Chen S. Microglia in neurodegenerative diseases: mechanism and potential therapeutic targets. Signal Transduct Target Ther. 2023;8(1):359.
101. Azmal M, Paul JK, Prima FS, Haque A, Meem M, Ghosh A. Microglial dysfunction in Alzheimer's disease: mechanisms, emerging therapies, and future directions. Exp Neurol. 2025;392:115374.
102. Leszek J, Barreto GE, Gasiorowski K, Koutsouraki E, Avila-Rodrigues M, Aliev G. Inflammatory mechanisms and oxidative stress as key factors responsible for progression of neurodegeneration: role of brain innate immune system. CNS Neurol Disord Drug Targets. 2016;15(3):329–36.
103. Wendeln AC, Degenhardt K, Kaurani L, Gertig M, Ulas T, Jain G, et al. Innate immune memory in the brain shapes neurological disease hallmarks. Nature. 2018;556(7701):332–8.
104. Warden AS, Wolfe SA, Khom S, Varodayan FP, Patel RR, Steinman MQ, et al. Microglia control escalation of drinking in alcohol-dependent mice: genomic and synaptic drivers. Biol Psychiatry. 2020;88(12):910–21.
105. Jiang C, Zhang Y, Tang X, Jing C, Qiu S, Li B, et al. IL-6 and IL-1beta upregulation and tau protein phosphorylation in response to chronic alcohol exposure in the mouse hippocampus. NeuroReport. 2021;32(10):851–7.
106. Grifasi IR, McIntosh SE, Thomas RD, Lysle DT, Thiele TE, Marshall SA. Characterization of the hippocampal neuroimmune response to binge-like ethanol consumption in the drinking in the dark model. NeuroImmunoModulation. 2019;26(1):19–32.
107. Gano A, Mondello JE, Doremus-Fitzwater TL, Deak T. Rapid alterations in neuroimmune gene expression after acute ethanol: Timecourse, sex differences and sensitivity to cranial surgery. J Neuroimmunol. 2019;337:577083.
108. Hommer DW. Male and female sensitivity to alcohol-induced brain damage. Alcohol Res Health. 2003;27(2):181–5.
109. Alfonso-Loeches S, Pascual M, Guerri C. Gender differences in alcohol-induced neurotoxicity and brain damage. Toxicology. 2013;311(1–2):27–34.
110. Patel RR, Varodayan FP, Herman MA, Jimenez V, Agnore R, Gao L, et al. Synaptic effects of IL-1beta and CRF in the central amygdala after protracted alcohol abstinence in male rhesus macaques. Neuropsychopharmacology. 2022;47(4):847–56.
111. Bajo M, Herman MA, Varodayan FP, Oleata CS, Madamba SG, Harris RA, et al. Role of the IL-1 receptor antagonist in ethanol-induced regulation of GABAergic transmission in the central amygdala. Brain Behav Immun. 2015;45:189–97.
112. Bajo M, Patel RR, Hedges DM, Varodayan FP, Vlkolinsky R, Davis TD, et al. Role of MyD88 in IL-1beta and ethanol modulation of GABAergic transmission in the central amygdala. Brain Sci. 2019;9(12):361.
113. Bajo M, Madamba SG, Roberto M, Blednov YA, Sagi VN, Roberts E, et al. Innate immune factors modulate ethanol interaction with GABAergic transmission in mouse central amygdala. Brain Behav Immun. 2014;40:191–202.
114. Garcia-Oscos F, Salgado H, Hall S, Thomas F, Farmer GE, Bermeo J, et al. The stress-induced cytokine Interleukin-6 decreases the inhibition/excitation ratio in the rat temporal cortex via trans-signaling. Biol Psychiatry. 2012;71(7):574–82.
115. Diaz MR, Barney TM, Marsland P, Deak T. Age- and cytokine-dependent modulation of GABAergic transmission within the basolateral amygdala of male Sprague Dawley rats. Neuropharmacology. 2025;267:110304.
116. Boyce EG, Rogan EL, Vyas D, Prasad N, Mai Y. Sarilumab: review of a second IL-6 receptor antagonist indicated for the treatment of rheumatoid arthritis. Ann Pharmacother. 2018;52(8):780–91.
117. Preuss CV, Anjum F. Tocilizumab. [Updated 2024 February 12]. In:StatPearls [Internet]. Treasure Island (FL): StatPearls Publishing.
118. Choy EH, De Benedetti F, Takeuchi T, Hashizume M, John MR, Kishimoto T. Translating IL-6 biology into effective treatments. Nat Rev Rheumatol. 2020;16(6):335–45.
119. Ridker PM, Rane M. Interleukin-6 signaling and anti-Interleukin-6 therapeutics in cardiovascular disease. Circ Res. 2021;128(11):1728–46.
120. Urban NB, Kegeles LS, Slifstein M, Xu X, Martinez D, Sakr E, et al. Sex differences in striatal dopamine release in young adults after oral alcohol challenge: a positron emission tomography imaging study with [(1)(1)C] raclopride. Biol Psychiatry. 2010;68(8):689–96.
121. Lingford-Hughes AR, Acton PD, Gacinovic S, Boddington SJ, Costa DC, Pilowsky LS, et al. Levels of gamma-aminobutyric acid-benzodiazepine receptors in abstinent, alcohol-dependent women: preliminary findings from an 123I-iomazenil single photon emission tomography study. Alcohol Clin Exp Res. 2000;24(9):1449–55.
122. Becker HC, Lopez MF. An animal model of alcohol dependence to screen medications for treating alcoholism. Int Rev Neurobiol. 2016;126:157–77.
123. Torres L, Tsirka SE. Sexual dimorphism of neuroimmune cells and its impact on the Central Nervous System: a special issue. J Pharmacol Exp Ther. 2020;375(1):152–3.
124. Nelson LH, Lenz KM. The immune system as a novel regulator of sex differences in brain and behavioral development. J Neurosci Res. 2017;95(1–2):447–61.
125. Chang GQ, Karatayev O, Boorgu D, Leibowitz SF. CCL2/CCR2 chemokine system in embryonic hypothalamus: involvement in sexually dimorphic stimulatory effects of prenatal ethanol exposure on peptide-expressing neurons. Neuroscience. 2020;424:155–71.
126. Chang GQ, Karatayev O, Halkina V, Edelstien J, Ramirez E, Leibowitz SF. Hypothalamic CCL2/CCR2 chemokine system: role in sexually dimorphic effects of maternal ethanol exposure on melanin-concentrating hormone and behavior in adolescent offspring. J Neurosci. 2018;38(42):9072–90.
127. Barton EA, Baker C, Leasure JL. Investigation of sex differences in the microglial response to binge ethanol and exercise. Brain Sci. 2017. https://doi.org/10.3390/brainsci7100139.
128. Mayfield J, Arends MA, Harris RA, Blednov YA. Genes and alcohol consumption: studies with mutant mice. Int Rev Neurobiol. 2016;126:293–355.
129. Turner NP, Bajo M, Roberts AJ, Roberto M, Yates JR, 3rd. The effects of alcohol dependence on the CSF proteome in mice: evidence for blood-brain barrier dysfunction and neuroinflammation. Neurobiol Dis. 2025;219:107254.
130. Ayata P, Crowley JM, Challman MF, Sahasrabuddhe V, Gratuze M, Werneburg S, et al. Lymphoid gene expression supports neuroprotective microglia function. Nature. 2025;648(8092):157–65.
131. Ayata P, Badimon A, Strasburger HJ, Duff MK, Montgomery SE, Loh YE, et al. Epigenetic regulation of brain region-specific microglia clearance activity. Nat Neurosci. 2018;21(8):1049–60.
132. Chahal SK, Kabra A. Fisetin ameliorates polycystic ovary syndrome in rats via a mechanistic modulation of AMP-activated protein kinase and SIRT1 molecular pathway. Naunyn Schmiedebergs Arch Pharmacol. 2024;397(12):10017–29.
133. Prabhala RH, Wira CR. Sex hormone and IL-6 regulation of antigen presentation in the female reproductive tract mucosal tissues. J Immunol. 1995;155(12):5566–73.

Publisher's Note